UNIVERSITY OF ESSEX

SCHOOL OF BIOLOGICAL SCIENCES

DATE OF SUBMISSION: 11TH JANUARY 2026

Inhibiting androgen receptor using decoy binding sites as a new treatment option for prostate cancer

A thesis submitted in accordance with the requirements of the University of Essex for the degree of MSD Cell and Molecular Biology

By Aliza Fowad

SUPERVISORS: Dr Greg Brooke & Dr Angela Pine

Statement of Originality

Unless otherwise stated in the text, this thesis is the result of my own work.

Acknowledgements

I would like to express my sincere gratitude to my supervisor, Dr Greg Brooke, for his exceptional mentorship. Whose guidance, expertise, and encouragement were instrumental throughout the course of this project and my MsD. His critical constructive feedback was essential for me at every stage of this research. I am also truly thankful to my second supervisor, Dr Angela Pine, for her support and insightful feedback at key stages of my research. My thanks extend to Dr Gareth Wright, my lab co-supervisor, whose practical knowledge in the lab environment made conducting experiments more manageable. I am also equally grateful to my lab colleagues for their constant support and willingness to help, and their humour made the long days in the lab genuinely enjoyable.

Finally, I would like to thank my family for being my foundation throughout this journey. Their unwavering belief in me, endless encouragement, patience and emotional support kept me grounded during both the highs and the challenges. This achievement is just as much yours as it is mine. Alongside this, I would also like to thank a special friend, Nadia, for being my unofficial thesis support system. Thank you for the constant encouragement, the laughs, positivity and for listening to endless thesis updates. Thank you for celebrating my achievements along the way and reminding me that there was more to life than experiments, corrections, and deadlines. We did this together. Consider this your official confirmation that you now hold an honorary MsD.

Abstract

The androgen receptor (AR) is a key driver of prostate cancer progression. Treatment options for prostate cancer target this pathway, but tumours invariably become resistant to these therapeutics. New treatment options are desperately needed for this treatment-resistant stage of the disease, where AR signalling remains active despite reduced androgen levels. This study investigated the use of decoy binding sites to inhibit AR signalling, using a mutated TAT-STOP plasmid containing indirect palindromic androgen response element (ARE) repeats. I hypothesised that ARE-based decoys could reduce AR-driven gene expression by competitively sequestering AR, irrespective of resistance mechanisms such as AR mutations or splice variants.

Site-directed mutagenesis was used to introduce a stop codon into the TAT-GRE-E1B-LUC plasmid, generating the mutated TAT-STOP construct. COS1 cells were co-transfected with either PSG5-EMPTY or the mutated TAT-STOP plasmid, and reporter assays were performed. These assays demonstrated a dose-dependent inhibition of reporter AR activity with increasing concentrations of TAT-STOP. With activity decreasing progressively and reaching approximately ~20% of MIB-treated control levels at 1000ng. Western blotting found that AR levels were lower in cells transfected with the TAT-STOP construct.

22RV1 cells, a model of therapy-resistant prostate cancer, were transfected with the TAT-STOP construct. qPCR analysis confirmed reduced AR signalling, evidenced by decreased expression of the AR-regulated genes *NDRG1* and *KLK2*. IncuCyte live-cell

imaging revealed suppression of MIB-induced proliferation in TAT-STOP-expressing cells, demonstrating a functional inhibition of androgen-driven growth. Ethanol-treated controls showed negligible proliferation, confirming androgen specificity. DNA nanoflowers were explored as a potential delivery strategy for the decoy binding site.

In conclusion, these data demonstrate that the mutant TAT-STOP plasmid acts as an effective decoy to inhibit AR signalling and AR-regulated gene expression. This supports ARE-based decoy strategies as a promising, resistance-agnostic therapeutic approach for AR-positive prostate cancer.

Abbreviations

1°: Primary

2°: Secondary

AR: Androgen receptor

ARE: Androgen Response Element

ARPIs: Androgen receptor pathway inhibitors

BBS**:** Borate Buffer Saline

Bp: Base Pair

cDNA: Complementary DNA

CRPC: Castrate Resistant Prostate Cancer

DBD: DNA Binding Domain

ddH_2O: Double distilled water

DHT: Dihydrotestosterone

DMSO: Dimethyl Sulphoxide

DNA: Deoxyribonucleic acid

dNTPs: Deoxyribonucleotides

dp: Decimal place

EDTA: Ethylenediaminetetraacetic acid

EtOH: Ethanol

FCS: Fetal Calf Serum

FBS: Fetal Bovine Serum

HCl: Hydrochloric acid

HSP: Heat Shock Protein

HSP: Heat Shock Proteins

kDa: Kilodaltons

LB: Luria- Bertani Broth

LBD: Ligand Binding Domain

LH: Luteinizing Hormone

LHRH: Luteinizing Hormone Releasing Hormone

MIB: Mibolerone

Min/s: Minute/s

mL: Millilitre

N-Terminal: Amino-Terminal

NaCl: Sodium Chloride

nm: Nanometre

nM: Nanomolar

Nt: nucleotides

PBS: Phosphate Buffered Saline

PCa: Prostate Cancer

PCR: Polymerase Chain Reaction

PSA: Prostate Specific Antigen

PSG: Polyglycerol Sebacute

PVDF: Polyvinylidene difluoride

RNA: Ribonucleic acid

Rpm: Revolutions per minute

RPMI: Roswell Park Memorial Institute

RT-PCR: Real Time PCR

RT: Room temperature

SDS-PAGE: Sodium Dodecyl Sulphate Polyacrylamide gel electrophoresis

SDS: Sodium Dodecyl Sulphate

siRNA: small interfering RNA

TAE: Tris/Acetic acid/EDTA

TBE: Tris/Boric Acid/EDTA

TE: Tris/EDTA

Tm: Melting temperature

TNM: Tumour, Nodes & Metastasis

Tris-HCl: Tris-Hydrochloric Acid

UV: Ultra violet

µg: micro gram

µL: micro litre

Table of Contents

List of Figures

List of Tables

Chapter 1: Introduction

1.0 Prostate cancer

1.1 Function of the Healthy Prostate Cancer

The prostate is an endocrine fibromuscular gland that plays a vital role in the male reproductive system. The gland is situated underneath the bladder and in front of the rectum, enclosing the urethra (Figure 1). As it is an endocrine gland, it secretes substances through the urethra. The prostate is anatomically divided into five lobes and histologically into distinct zones. The gland predominantly consists of 70% glandular and 30% fibromuscular tissue (William K. Oh, 2003) and 3 main zones: the transition zone (the smallest region), the central zone where the ejaculatory duct is located and the peripheral zone where prostate cancer (PCa) is most likely to develop (McNeal, 1981).

Consisting of 70% glandular tissue, the peripheral zone is responsible for producing the prostatic fluid, which is necessary for male fertility and equates to approximately 25% - 30% of the total volume of semen. The composition of this fluid is mainly enzymes, spermine, zinc and citric acid. All of these contribute to sperm nourishment and act as an essential energy source for sperm cells, assisting in sperm viability and therefore impacting fertilisation (Mann, 1974). Alongside its role in semen production, the prostate gland contributes to local androgen signalling through tissue- specific conversion of testosterone to its active form of dihydrotestosterone

(DHT), which is important for maintaining normal prostate function (Page et al., 2011).

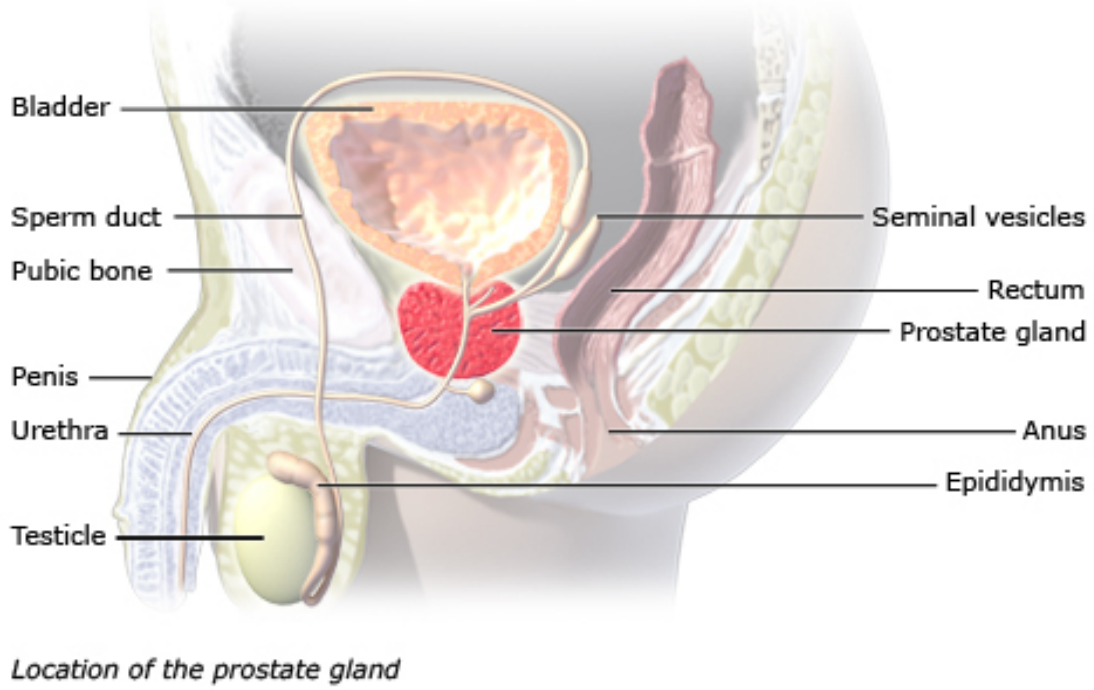

Figure 1- Male reproductive system: Location of the Prostate Gland

Demonstrating the male reproductive system (image taken from How Does the Prostate Work, 2022).

1.1.1 Prostate Cancer

Cancer is referred to as a group of diseases that can develop from anywhere in the body, characterised by the uncontrollable spread and growth of abnormal cells (NIH, 2021). Similarly, PCa is typically derived from a single abnormal cell in the prostate gland; arising as the cells normal control mechanisms are compromised and thus, they have the ability to grow and multiply continuously. PCa is the most prevalent cancer type in men in the UK, and approximately 1 in 8 men will be diagnosed with

the disease in their lifetime, equating to 52,000 patients per year and 490,000 men worldwide (CRUK 2022).

PCa cells possess the ability to invade surrounding tissues and nodes, migrate and metastasise to other sites of the body. As these abnormal cancerous cells grow and divide, they begin to form a mass of tissue known as a tumour (Gale, 2024), which via invasion, destroys normal adjacent tissues, also known as malignant tumours. Tumours are categorised into two categories: benign tumours typically stay stationary in their primary location and do not invade into neighbouring tissues. In contrast, malignant tumours are known as cancerous and can invade surrounding tissues and metastasise to other sites through the bloodstream or the lymphatic system. PCa cells are known to invade sites like bones, lungs and lymph nodes surrounding the pelvis. Pelvic lymph nodes are situated alongside the iliac arteries (Datta et al., 2010), and their main function is to drain and filter lymph from nearby areas.

1.1.1.1 Prostate Cancer Risk Factors and Diagnosis

Several scientifically proven risk factors have been shown to contribute to the development of PCa. Some of which are family history of PCa, genetics, age, ethnicity, sexual activity, diet and infections. Studies have demonstrated that age is also a significant risk factor for the disease; risk increases as a male reaches the age of 55 (Gann, 2002) and tends to rapidly increase until 70 years and slightly declines after. Studies have also shown that acinar adenocarcinomas are the most frequently found tumour growth related to PCa that develops from the peripheral prostatic gland, making up 90-95 % of all diagnosed cases (Murray, 2021, Lee et al., 2015).

Detecting and diagnosing PCa cannot be carried out via a single definitive test. Instead, a combination of examinations are performed to effectively diagnose the disease. These may involve a blood test for prostate-specific antigen (PSA), which is commonly paired with an MRI scan if PSA levels are increased. If there is suspicion of a tumour, a biopsy may be performed to confirm the diagnosis and to assess the aggressiveness of the disease. Patients presenting with specific PCa-related symptoms, like urinary difficulties or haematuria, can also undergo a digital rectal examination (DRE) to assess for any abnormalities in the gland.

Early detection of PCa is beneficial as the disease tends to be more localised. If caught whilst the tumour is organ-confined, better treatment options are available, including the option of active surveillance (Dahabreh et al., 2012). Delays in the diagnosis process could result in different treatment options, as the tumour cells would have gone undetected for a prolonged period and could have spread to surrounding areas. In such cases, the clinical management of the disease becomes more difficult as surgery is no longer an option.

1.2 Androgen Receptor and Androgen Hormones

Androgens are crucial C19 steroid hormones that are important in the development of the male sexual characteristics, and the main circulating androgen is testosterone (Tan et al., 2015). Androgen receptor (AR) is a steroid receptor and a ligand-dependent transcription factor (Brinkmann, 2011) that mediates the action of androgens such as testosterone and 5α-dihydrotestosterone.

Androgen signalling supports the proliferation and survival of prostate-driven cancer cells and therefore contributes to prostate cancer progression. Due to AR signalling, the growth of cells is often driven by androgens acting through the AR in a DNA-binding dependent manner (Davey and Grossmann, 2016). As a result, this pathway is often targeted for the treatment of PCa, through e.g. the use of antiandrogens. Antiandrogens are ligands that can inhibit the action of the AR by binding to the receptor and holding it in an inactive state (Brooke and Bevan, 2009).

1.2.1 Androgen Receptor Structure

Nuclear Receptor subfamily 3, group C, gene 4 (NR3C4) is the name given to the gene that encodes the AR. The gene consists of 8 exons and is located at Xq11.2-12 of the X chromosome (Figure 2). Since males have one X chromosome, they possess a single copy of this gene. Therefore, any genetic modification altering the expression of the AR protein can affect androgen signalling . (McEwan, 2021).

The AR consists of four distinct domains that aid in carrying out its functions. In order of 5' to 3', the first domain is the NH2-terminal domain (NTD) coded by exon 1, which houses activation function 1 (AF-1) that is needed for transcriptional activity. The domain is important in the recruitment of transcriptional complexes (Narayanan et al., 2008) and also interacts with the ligand-binding domain (LBD), stabilising the AR dimer complex and ligand-receptor complex. The central zone contains the DNA-binding domain (DBD), which is responsible for the specific DNA binding to androgen response elements (AREs) (Fujita and Nonomura, 2019). The AREs are responsible for regulating the expression of androgen-responsive genes. Any anomalies like mutations in the DBD (e.g. as seen in some cases of androgen insensitivity syndrome), can disrupt DNA binding, inhibiting androgen signalling (McEwan, 2021).

Acting as the linker, the hinge region is located between the DBD and LBD and is encoded by exon 4. The hinge region contains a nuclear localisation signal and a co-repressor binding domain. The C-terminal region (exons 5-8) contains the ligand-binding domain, which is where androgens like testosterone and dihydrotestosterone bind. Ligand binding promotes conformational changes (Brinkmann et al., 1999) to activate the receptor and regulate target gene expression.

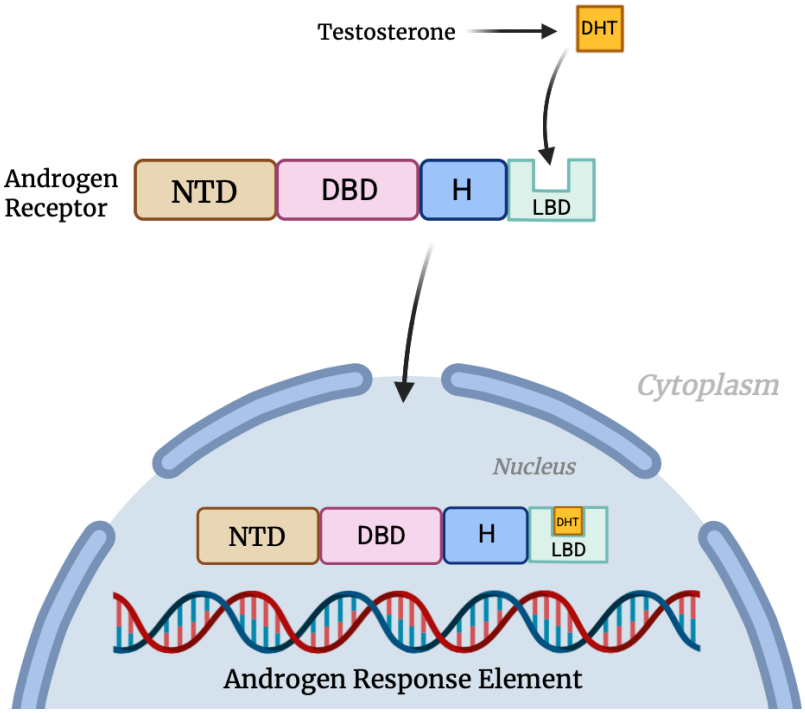

Figure 2- Androgen Receptor Pathway:

Schematic illustrating the androgen receptor (AR) domains and a summary of the signalling pathway. Testosterone is converted to dihydrotestosterone (DHT), which binds to the ligand-binding domain (LBD) and initiates and promotes androgen receptor translocation into the nucleus, where AR binds to androgen response elements (AREs) to regulate gene transcription. Androgen receptor domains shown (left to right) include the N-terminal domain (NTD), DNA-binding domain (DBD), hinge region (H), and the ligand- binding domain (LBD). Figure generated using Biorender.

1.2.1.1 Androgen Receptor Pathway

The androgen receptor pathway is a series of events that lead to the regulation of gene expression (Aurilio et al., 2020). Testosterone is produced in the testes and circulates in the body through the bloodstream. Testosterone crosses the membrane

of the target cell and is converted to the more active form dihydrotestosterone (DHT) by the enzyme 5α-reductase (McEwan, 2021). In the absence of androgen, AR resides in the cytoplasm of the cell (Figure 3). When unbound, the AR binds to heat shock proteins (HSPs) to stabilise the receptor and hold it in a ligand-binding competent state. Upon entering, DHT binds to AR, causing a conformational change which dissociates the HSPs. This results in the unmasking of the nuclear localisation signal (NLS) in the AR hinge region, translocation to the nucleus and dimerisation. Upon entering the nucleus, the AR complex interacts with AREs in the regulatory regions of target genes. Following ligand binding, the AR undergoes co-regulator recruitment, and gene transcription can either be enhanced or repressed via the recruitment of coactivators or corepressors. These interactions determine if target genes are suppressed or activated (McEwan, 2021).

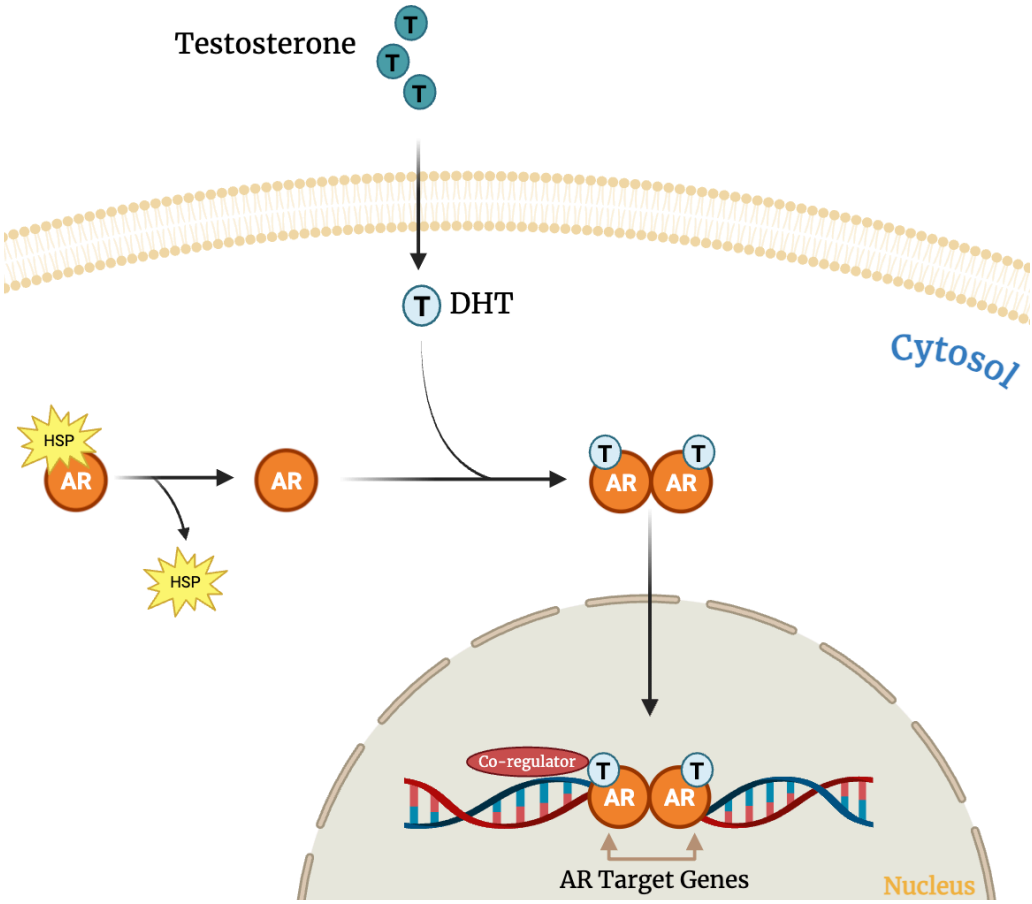

Figure 3- Androgen Receptor Signalling Pathway

Schematic representation of the androgen genomic pathway. In the cytoplasm, the androgen (testosterone) is converted to dihydrotestosterone (DHT) and binds to AR. The androgen receptor is activated, dimerises, and translocates into the nucleus to bind to specific DNA sequences. Co-regulators assist the AR with transcription of target genes. Figure generated using Biorender.

1.2.1.2 Androgen Production

It is known that the initiation of PCa is heavily reliant upon androgens. These hormones are responsible for the maintenance and development of male characteristics. Both men and women express androgens, however, in different sites in the body. Males produce androgens in the Leydig cells in the testes, metabolised from cholesterol and secreted as testosterone. Females predominantly produce androgens from the ovaries and secreted as dehydroepiandrosterone (DHEA).

Testosterone production is closely linked with the hypothalamic-pituitary-gonadal axis; gonadotropin-releasing hormones (GnRH) release leads to the secretion of luteinizing hormone (LH) (Tolkach et al., 2013). The regulation of testosterone is initiated when the LH acts on the Leydig cells located in the testes (Zirkin and Papadopoulos, 2018), promoting testosterone production. This applies a negative feedback loop on the hypothalamus, reducing GnRH synthesis (Figure 4).

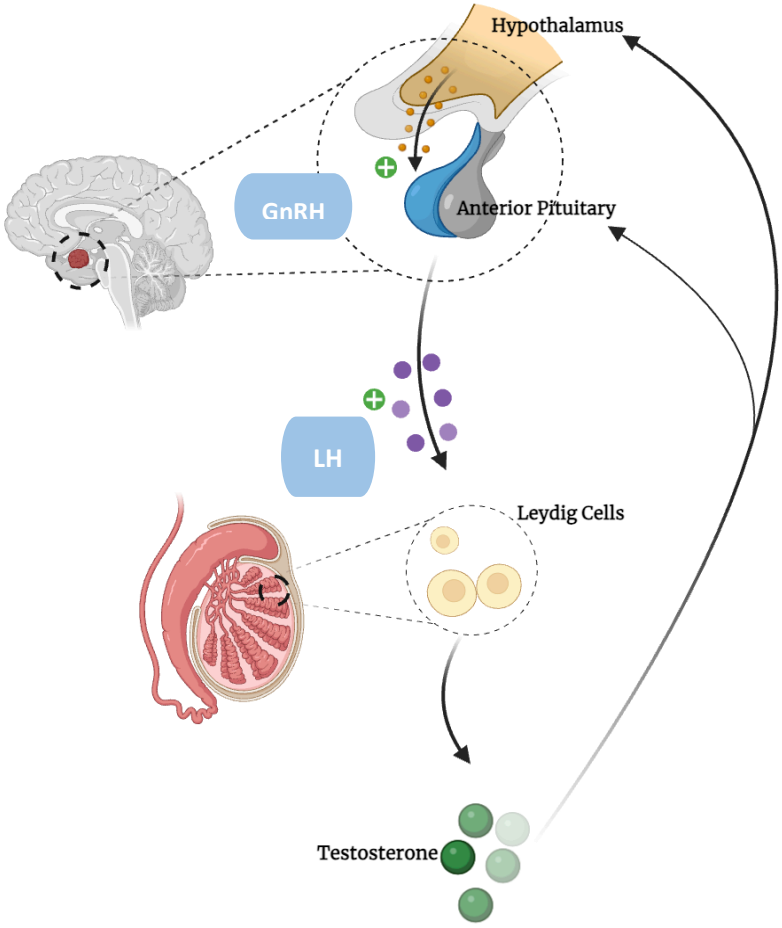

Figure 4- Testosterone Production Pathway

Schematic illustration of testosterone production. The hypothalamus secretes gonadotropin-releasing hormones (GnRH), activating the pituitary gland to secrete luteinizing hormone (LH). LH sends a signal to the Leydig cells promoting testosterone production. This signals a negative feedback loop on the hypothalamus. Figure generated using Biorender.

1.3 Treatment Options for Prostate Cancer

Currently, there is a variety of effective treatments available for treating PCa. However, every treatment is dependent on individual circumstances such as the presence/absence of metastasis, stage and grade of the cancer and the general health of the male. The long-term goal for treatment is to primarily help minimise and control the growth of the cancer, therefore, ultimately extending life expectancy. Conversely, in cases where the cancer has metastasised and developed into later stages, the treatment plan may focus more on delaying, improving symptoms and prolonging life.

Early detection offers less invasive treatment options. Upon examination results, if tumours are predicted to grow slowly, they are scored as 'low grade'. In this case, healthcare specialists advise following the watchful waiting and active surveillance approach. This method is commonly advised to older patients (NHS,2024) as the cancer is less likely to affect their natural life expectancy. Patients who already have health implications may be recommended to avoid undergoing any invasive treatments. Active surveillance is the approach used for patients with low-risk cancers, avoiding any unnecessary treatment. Routine tests like MRI scans, biopsies and PSA tests are recommended to keep track of any cancer progression. Any advancements in treatment will be dependent on the outcome of these tests (Coen et al., 2011).

LHRH agonist (buserelin, goserelin) and androgen synthesis inhibitor (abiraterone, orteronel) (Yamaoka et al., 2012) are drugs that have been through clinical practice and have been shown to be effective in suppressing testosterone and other androgen levels. Anti-androgens such as galeterone (TOK-001), nilutamide, flutamide and bicalutamide act through a similar mechanism by competitively binding to the AR thereby preventing activation by testosterone and dihydrotestosterone (DHT) and reducing androgen signalling (Shet et al., 1997). As a result, androgen receptor-mediated stimulation of prostate cancer cell growth is reduced. (introduction)

1.3.1 Invasive/Systemic Treatment Options

Some patients may present with cancer in the prostate alone. An invasive procedure known as radical prostatectomy can be performed to remove the prostate gland. Other treatments like radiotherapy and hormone therapy are combined to control and minimise the progression of the cancer (NHS, 2024). Advanced treatments such as androgen receptor pathway inhibitors (ARPIs) and radioligand therapy (PSMA-targeted therapy) are recommended when the cancer has progressed to its later stages, and is impossible to cure, but is possible to slow down its progression. Advanced prostate cancer is often treated by bypassing or suppressing androgen signalling rather than eliminating the tumour.

1.3.1.2 Castrate Resistant Prostate Cancer

As PCa requires the hormone testosterone to grow, treatment is delivered to completely inhibit and block the supply of testosterone via androgen deprivation therapy (ADT). Castrate resistant prostate cancer (CRPC) is the name given to advanced PCa that continues to grow despite ADT. Androgen deprivation therapy aims to lower testosterone levels to reduce the cancer's growth. Hence, the cancer is thought to have become resistant to treatment like hormone therapy. CRPC is typically categorised and diagnosed by disease progression and comes in two forms, metastatic and nonmetastatic. Metastatic CRPC is where the cancer has migrated to other regions in the body, thus accounting for the highest number of PCa patient deaths. Treating with ADT is not recommended as the cancer has adapted to grow and developed into its castration resistant transient form (Karantanos et al., 2013).

1.3.1.3. Advancements on Treatment

Recent and ongoing research is significantly advancing treatment options for PCa. For example, there have been advancements in developing vaccines as a therapeutic intervention for the disease. Sipuleucel-T is a prostate antigen-specific autologous cellular vaccine that is FDA-approved for treatment (Madan and Gulley, 2011). Being especially effective in advanced prostate cancer cases such as metastatic castration-resistant prostate cancer (mCRPC). It primarily works to stimulate immune cells that are capable of targeting PCa cells to either eliminate recurring disease or delay cancer progression. Approaches related to vaccines have been studied (Rastogi et al.,2023); however, they displayed poor clinical evidence in activity as a single treatment option. As described above, androgen signalling drives and promotes prostate cancer

growth. In most cases (Saranyutanon et al., 2019), developments of AR signalling have been targeted at exploiting the idea of targeting the AR receptor and the ligand. However, recent clinical practices are exploring alternative strategies that aim to indirectly suppress AR signalling through targeting its co-factors. The theory of interference with the interaction of AR with its cofactors has been explored. Studies suggest that onalespib, a small molecule drug that has potential in targeting and inhibiting the heat shock protein 90 (HSP90), leading to degradation of AR and other proteins (Ferraldeschi et al., 2016). It was demonstrated that AR variant 7 (AR-V7) and AR full l4ength (AR-FL) were both depleted upon the introduction of inhibition of HSP90.

Advancements in novel therapies for castrate resistant prostate cancer (CRPC) have been progressing. A thorough understanding of the molecular biology behind CRPC (Garcia and Rini, 2012) has led to an unexpected shift in treatment for patients with metastatic disease. Several novel strategies to target the AR have been developed, including decoy binding sites.

1.4 Decoy Binding Sites

Although there are successful treatments for prostate cancer, therapy resistance is common and therefore, new therapeutic strategies are needed. Therefore, alternative strategies directly targeting AR signalling are being explored. Decoy binding sites are a promising potential approach that can be used to target oncogenic transcription factors. Decoy binding sites are artificially assembled constructs that aim to mimic natural AREs, blocking the AR from binding to the regulatory regions of target genes (Myung et al., 2017). Prior research has indicated that applying synthetic ARE

decoys could effectively inhibit AR downstream gene expression and AR activity by reducing the interaction between the receptor and endogenous response elements. Thereby, leading to reduced transcription of regulated genes like prostate-specific antigen (PSA) in PCa cells (Cleutjens et al., 1997).

Decoy binding sites can come in the form of transcription factor decoys and receptor decoys. Receptor decoys typically function by intercepting the hormone, in this case, androgen, from binding to the AR (Wang et al., 2021).

Androgen receptor DBD decoy molecules specifically for PCa have been developed. Decoy molecules stemmed from the AR N-terminal domain (Quayle et al., 2007) to limit its activity. Existing evidence proved that *in vivo* expressions of AR NTD decoys reduced tumour growth and tumour incidences, inhibiting cancer growth. Demonstrating a 4-fold decrease in tumour volume and a significant (Visakorpi et al., 1995) 10-fold decrease in serum prostate-specific antigen (PSA). Cell viability assays demonstrated that cells treated with AR NTD decoys underwent apoptosis and had reduced proliferation. No change was detected in the cells that were AR independent. This study highlights the importance of the N-terminal domain within the AR in the progression and growth of prostate cancer.

Androgen receptor elements are used in the decoy binding approach (Aulakh and Mysore, 2025). AREs are comprised of short DNA sequences to which the androgen receptor attaches and binds to in order to fully activate genes involved in prostate cancer cell growth. In the presence of androgens like testosterone, AR binds to

available AREs in the promoter of target genes, switching them on. In decoy sites, the AR binds to decoy AREs instead of binding to real genes, preventing the AR from switching target genes to their active state. Androgen receptor signalling is reduced regardless of whether AR is mutated or is present in another variant form. In the case of prostate cancer, some cancers develop resistance due to AR mutations, so AR signalling is still widely used. ARE-based decoy sites do not rely on blocking the ligand binding site, allowing them to work when other conventional therapies fail.

1.4.1 Targeted delivery of novel therapeutics

Studies have highlighted potential delivery approaches like nanoparticle encapsulation and DNA nanoflowers (DNFs), which show promising results in enhancing the stability of nucleic acid-based therapeutics and cellular uptake in cancer models. In nanoparticle-mediated delivery, the drug is trapped within tiny carrier materials, such as liposomes, and aptamers can be included to target the cancer cells (Fu and Xiang, 2020). Targeted delivery also occurs as nanoparticles start to gather and leak into tumours via the enhanced permeability and retention effect (EPR effect). This strategy aims to enable controlled release of the therapeutic, with reduced off-target effects (Jiang Zhao, 2022). Early pre-clinical trials are currently underway for improving targeted tumour drug delivery and for reducing toxicity, and are showing promising results in animal models where tumour reduction and improved survival has been identified (Jiang Zhao, 2022).

1.4.1.1 DNA Nanoflower and Delivery

A potential delivery option for DNA-based therapeutics is DNA nanoflowers. DNFs are flower-shaped nanomaterials that are synthesised through rolling circle amplification (RCA, Figure 5). A circular DNA template is amplified by DNA polymerase, creating long repetitive strands that assemble into flower-like structures called nanoflowers. The production of DNFs can be modified, resulting in differences in overall shape, size and functional elements such as decoy sequences and aptamers. DNA nanoflowers can be designed to include aptamers, allowing for targeted delivery (Jigang Lv, 2020)

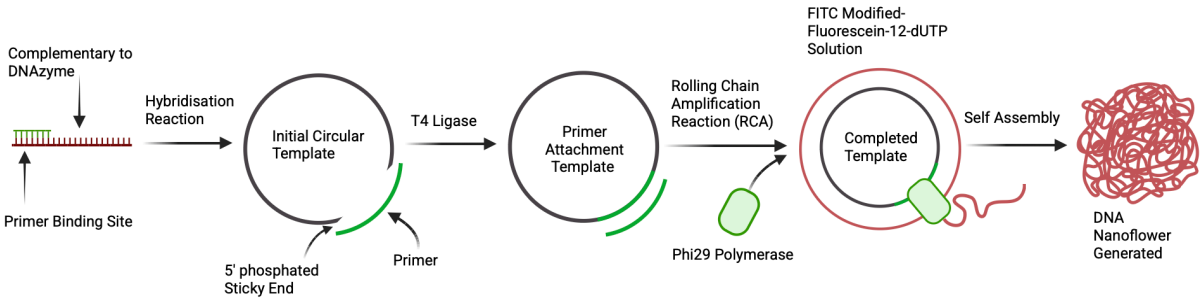

Figure 5. Synthesis of DNA nanoflowers.

Schematic diagram summarising the synthesis of DNA nanoflowers. The primer is complementary to the DNA strand, and upon annealing and ligation, forms a ring-like structure. The Phi29 enzyme is used for the rolling circle amplification process and attaches to the template, generating a long chain of DNA, which assembles itself into a stable DNA nanoflower. Figure generated using Biorender

To investigate the potential delivery approach for the decoy delivery, androgen response elements (AREs) sequences from the TAT-GRE-E1B-LUC and TAT-STOP constructs were incorporated into DNA nanoflower (DNF) templates. The ARE decoys regions were the only ones retained. The luciferase gene and non-essential plasmid sequences were excluded. Both direct and palindromic ARE repeat sequences were investigated to determine their effect on DNA nanoflower (DNF).

DNA nanoflowers formation occurs through spontaneous self-assembly of long DNA products that are generated during rolling chain amplification (RCA). This is driven by sequence repetition and accumulation of DNA-magnesium pyrophosphate complexes, byproducts produced during synthesis. The AREs sequences were incorporated into the circular template design before amplification, enabling repeated generation of the decoy binding motifs throughout the developing nanoflower structure.

Research Aims

Prostate cancer growth is primarily driven by AR signalling. Although AR-targeted therapies are effective, resistance frequently occurs, often through persistent AR activity and AR variants that are constitutively active. Hence, this research aims to test whether exogenous androgen response elements (AREs) can function as competitive decoys to deter AR away from endogenous promoters and reduce and/or inhibit AR-dependent transcription. A secondary aim was to generate nanoparticles containing the decoy sites and assess their activity in cells. PCR will be performed to generate nanoparticles containing the response elements. The nanoparticles will be added to cells, and uptake will be confirmed using fluorescent microscopy.

The Aims are as follows:

1) **Establish reporter assay conditions for quantifying AR activity.**

   COS1 cells will be used to optimise androgen stimulation using different mibolerone (MIB) doses.

2) **Generate and validate a non-functional reporter construct for decoy competition experiments.**

   Site-directed mutagenesis will be used to introduce a premature stop codon into the luciferase sequence of TAT-GRE-E1B-LUC, creating the TAT-STOP construct. The stop codon will be introduced to prevent functional luciferase expression while maintaining the androgen response element binding sequence. Unlike the TAT-GRE-E1B-LUC plasmid, the TAT-STOP construct will

be designed to compete for androgen receptor binding without outputting reporter activity.

The mutation will be confirmed by Sanger sequencing and BLAST alignment. Functional validation will be performed using reporter assays

3) **Determine whether the ARE-containing decoy construct suppresses AR-dependent transcription in COS1 cells**

   COS1 cells will be co-transfected with plasmids for the AR, TAT-GRE-E1B-LUC, and TAT-STOP constructs.

4) **Test whether the decoy inhibits endogenous AR signalling and AR-dependent proliferation in 22RV1 cells**

   Transfection efficiency will be assessed by GFP fluorescence imaging. Proliferation will be measured by live-cell imaging and confluency measurements. qPCR will quantify AR target gene expression in response to the decoy.

5) **Investigate DNA nanoflowers as a potential delivery for ARE decoy sequences**

   DNFs containing direct or palindromic ARE sequences will be generated by rolling circle amplification and assessed using EVOS fluorescence microscopy across multiple reaction time points.

Chapter 2: Materials and Methods

2.0 Reagents, buffers and solutions

Table 2.1: List of reagents, buffers and solutions

Name	Description	Storage & Sterilisation
Bacterial work		
Ampicillin	1 g sodium ampicillin, ddH_2O to 10 mL	○ -20°C ○ sterilised filter tips. ○ 0.2 μm filter pore
Luria Broth (LB)	10 g Sodium chloride (NaCl), 10 g bactotryptone, 5 g yeast extract per 1 litre of RO water. Supplemented if required using 100 μg / mL of ampicillin (Sigma).	○ RT ○ Autoclaved
Glycerol Samples/stocks	Bacterial glycerol samples are used to grow bacteria.	○ -70°C ○ Collected with sterilised tips
SOC Medium	4 g tryptone, 1 g yeast extract, 0.1168 g 10 mM NaCl, 0.0372 g 2.5 mM KCl, ddH_2O to 200 ml, 0.1904 g 10 mM $MgCl_2$, 0.7206 g 20mM glucose	○ RT ○ Autoclaved
DNA agarose gel electrophoresis		
Agarose Gel (1%)	1 g agarose dissolved in 100 mL of 1 X Tris Acetic acid Ethylenediaminetetraacetic acid (EDTA) (TAE) via boiling and 5 μL of ethidium bromide (1 μg/mL).	○ Gloves when handling gel ○ RT or gels can be wrapped and stored at 4°C overnight.
Tris Acetic acid EDTA (TAE) (1X)	40 mM Tris, 20 mM acetic acid and 1 mM EDTA.	○ RT

Passaging, Culturing and Treating cells		
DMEM, (Dulbecco's Modification of Eagle's Medium) with 4.5 g/l glucose, L-glutamine & sodium pyruvate	Gibco FBS, 25ml Foetal calf serum (FCS) (10%) and 5ml Penicillin- Streptomycin-Glutamine (PSG) (10%) added into a 500 ml bottle of medium.	○ 4°C
0.05% Trypsin, 0.53 mM EDTA, 1X [-] sodium bicarbonate	0.5 ml of trypsin was used to detach COS cells from bottom of flask	○ 4°C
DMEM, 1X (Dulbecco's Modification of Eagle's Medium) with 4.5 g/l glucose, L-glutamine & sodium pyruvate without L-glutamine & phenol red.	12.5ml Stripped FCS (sFCS) (5%) (charcoal stripped) and 5ml Penicillin-Streptomycin-Glutamine (PSG) (10%) added into a 500 ml bottle of medium.	○ 4°C
PBS (Phosphate Buffered Saline)	Used to wash cells before trypsin (0.5 ml) is applied.	○ RT
Chemgene	Used as a disinfectant to clean surfaces and equipment.	○ RT
DMEM, 1X (Dulbecco's Modification of Eagle's Medium)	Gibco sFBS, and PSG added into a 500 ml bottle of medium (stripped, yellow in colour).	○ 4°C

with 4.5 g/l glucose, L-glutamine & sodium pyruvate, phenol red-free		
EtOH	Treatment used as a control.	○ -20°C
Mibolerone (7α,17α-dimethyl-19-nortestosterone)	Mibolerone, dissolved in Ethanol (10nM) was used as a synthetic androgen steroid.	○ -20°C

2.1 Cell Culture

2.1.1 Passaging cells

COS1 cells, derived from CV-1 monkey kidney cell line, were cultured in a humidified incubator with 5% CO_2 levels at 37°C. The cells were grown in DMEM, 1X medium supplemented with 10% Foetal Calf Serum (FCS) plus PSG. Cells were passaged once ~ 80% confluency was reached, mostly twice a week. Then, cells were washed with 10 ml PBS, and trypsinised with 0.5 ml trypsin and incubated for a few minutes at 37°C to detach the cells from the flask. 9.5 ml of DMEM was used to resuspend the cells, and 3 ml of the cell suspension was added to a fresh flask containing 15 ml of media. The flask was incubated at 37°C until confluent again.

2.1.2 Setting up 24-well plates

Cell suspension containing 50,000 cells per mL was prepared by adding 2.5 mL of cell suspension (see section 2.1.5) to 22.5 mL of stripped media. A total of 1 ml was seeded into each well of a 24-well plate. Cells were incubated for 24 hrs before transfection.

2.1.3 Transfection -24 well plates

Cells in 24-well plates were transfected with a master mix containing the following plasmids pSVAR (50-100 ng), BOS-β-GAL (100 ng), TAT-GRE-E1B-LUC (250-2000 ng) to a total volume of 45 µl with ddH_2O. Per well, 5 µl of $CaCl_2$ and 50 µl of BBS (Borate Buffer Saline), a buffered solution used to maintain pH levels during transfection, were added to the final master mixes and, with a pipette, bubbled to mix. Prepared master mixes were left to rest at RT for 15 minutes. Finally, 100µl of each master mix was added to the corresponding wells in the 24-well plates.

2.1.4 Treatment of Cells

Media was removed from the wells, and the cells were washed twice with 1ml of PBS (Phosphate Buffered Solution), a buffered salt solution used to wash cells and remove residual media. EtOH and MIB were diluted in media to a final concentration of 10 nM, and 1 ml was added per well. Cells were incubated for a further 24 hrs before cell harvesting.

2.1.5 Cell Counting and Plating

Following trypsinisation, 10 μL of cell suspension was taken from the flask and pipetted onto and viewed on a haemocytometer. To calculate the cell concentration, the cells/mL = average cell count per square ($1mm^2$) x 10^4 x dilution factor calculation was used.

2.1.6 Freezing and Defrosting Cells

To prepare frozen cell stocks, cells were cultured, passaged and pelleted via centrifugation. Cell pellet was resuspended in a freezing medium solution consisting of 90% fetal bovine serum (FBS) AND 10% dimethyl sulphoxide (DMSO Sigma). The mixture was placed into a cryotube and wrapped in appropriate insulating material and stored at -80 ^{o}C. overnight.

To defrost frozen stocks, the frozen cells were defrosted in warm water and transferred into 10 ml of incubated medium. The cell suspension was centrifuged at 2000 rpm for 5 minutes, and the supernatant was removed. The cells were resuspended in 10 mL of incubated medium. Cell suspension was transferred into a 75 mL culture flask, and additional medium was added to make 15 mL of total medium. Cells were left to incubate overnight.

2.1.7 Luciferase and β-gal Assays

Following 24 hours of treatments (see section 2.1.4.), COS1 cells were washed twice with 1 ml chilled PBS per well, and 60 μl of reporter lysis 1x buffer (Promega) was added per well. The plates were frozen at -80°C for 15 minutes and then defrosted at RT. For the β-galactosidase assay, 5 μl of lysate from each corresponding well was

transferred into a white 96-well plate together with 50 μl of β-gal reagent (Tropix® Galacto reaction buffer and 1:100 mix of Tropix®), covered with foil and left to mix on a shaker at RT for 1 hour. After 1 hr, 75 μl β-gal accelerator was added to each well, and the plate was left on a shaker at RT for a further 15 minutes. For the luciferase assay, 20 μl of lysate was transferred into a white-walled 96-well plate, and 20 μl of luciferase substrate (Promega) was added. The plate was left on a shaker at RT for 15minutes. Luciferase and β-galactosidase activity were measured using a CLARIOstar Plus plate reader.

2.2 Bacterial Transformations and Culture Preparation

2.2.1 Inoculation of Bacterial Culture

5 ml of LB was added to a sterile tube, and ampicillin (Amp) was added to a final concentration of 100 μg/ml. The LB was inoculated with bacteria from glycerol stocks and cultures incubated overnight at 37 °C with shaking at 180 RPM.

2.3 Plasmid Preparations

2.3.1 Midi/Maxi Preparation

For large-scale plasmid, Plasmid Purification Midi/Maxi kits (Qiagen Plasmid Plus Maxi Kit, Germany) were used, following the manufacturer's protocol. Bacteria were pelleted (4000 rpm for 10 minutes) and the supernatant removed. The pellet was resuspended in 8 mL P1 buffer (chilled with + lyse blue) and tubes inverted 4-6 times. Following this, 8 mL of buffer P2 was added, and the tubes were inverted until the lysate appeared viscous. The tubes were subsequently incubated at RT (15-25°C) for 3 minutes. 8 mL of buffer P3 was added, and the tubes were immediately inverted

until the solution turned colourless, followed by a 10 min incubation at RT. The tubes were centrifuged at 4000 rpm for 10 min, and the supernatant was filtered through a filter cartridge. Following this, the QIAvac 24 plus was prepared by inserting the QIAGEN Plasmid Plus columns. 5 mL of buffer BB was added to the cleared lysate, and the lysate was passed through a midi-/maxi-prep column using vacuum. The column was washed with 7 mL of buffer ETR. To completely remove residual wash buffer, the maxi spin column was placed into a 2 mL collection tube and centrifuged in a tabletop microcentrifuge (Eppendorf™ Minispin™/MiniSpin™ plus Centrifuge) at max speed (13000 rpm) for 1 minute. To elute, the column was placed in a clean Eppendorf, and 200 µl or 400 µl (midi-prep/maxi-prep) of distilled water was added to the centre of the column. The tube was incubated for 1 minute, centrifuged (Eppendorf™ Minispin™/MiniSpin™ plus Centrifuge) at max speed (13000 rpm) for 1 minute. An ND-1000 UV/VIS Spectrophotometer was used to measure the purity and concentration of the sample.

2.4 Immunoblotting/ Western Blots

2.4.1 Gel Preparation (SDS-PAGE)

For the resolving gel, 3.35 ml of ddH_2O, 3.75 ml of 1.0 M Tris pH 8.9, 100 µl of 10% SDS, 100 µl of 10% APS and 3.3 ml of 30 % Acrylamide were combined before the addition of 10 µl of Temed **(**Tetramethylethylenediamine)**.** The solution was poured into the glass plates, 0.5 ml of water saturated butanol was added, and the gel was left to set at RT for 30-40 min. For the stacking gel, 2.17 ml of ddH_2O, 1.88 mL of 1.0 M Tris pH 6.8, 50 µl of 10% SDS, 50 µl of 10% APS, and 0.85 mL of 30% Acrylamide was combined before the addition of 5 µl of Temed. The stacking solution

was added above the resolving gel, and a comb was inserted (10 or 15-well comb, depending on sample number).

2.4.2 Immunoblotting Procedure

Lysate from reporter assays were sonicated (Biorupter - 2 min, 30 sec on/off, high power) and spun at max speed for 10 min, 4 °C. Supernatants were transferred to fresh tubes and protein concentrations measured using a Nanodrop. 40 μg of each sample was added to a fresh tube and combined with 6 x loading dye. Samples were boiled for 5 min before use. Gels were run at 100 V for 1 hr to 1.5 hrs. Following this, the gels were removed and soaked in 20% ethanol. Next, using the iBlot gel transfer machine (Invitrogen. Thermo Fisher Scientific) at setting 7, the proteins were transferred onto a nitrocellulose membrane, blocked in 5% milk PBS-T (0.1% Tween) and left to rotate at RT for 30 minutes. Blots were probed with antibodies specific for the androgen receptor (ER179, Abcam) and α-tubulin (11224-1-AP, Proteintech); left to rotate at RT for 1 hr. The blots were washed quickly 2x with PBS-T, followed by 3 x 5 mins washes with PBS-T with rotation. The blots were re-blocked for 5 min before the addition of secondary antibody (HRP-conjugated Goat Anti-rabbit IgG (H+L)) and left to rotate at RT for 1 hour. The blots were washed as described previously with an additional PBS wash. To visualise AR, 500 µl of luminol/enhancer solution and 500 µl of stable peroxide solution ECL (enhanced chemiluminescence substrate), for tubulin detection, 1 ml of Luminata Forte Western HRP Substrate was added to the blots and membranes visualised using a LiCOR system.

2.5 RNA Extraction, Reverse Transcription and qPCR

Cells were seeded. In 6 well plate, transfected with the STOP-LUC plasmid, treated ± MIB and incubated for 24 hrs. Total RNA was extracted using a Monarch (New England Biolabs) RNA miniprep kit, and concentrations and purity was quantified using a Nanodrop. 250 ng of RNA was used for reverse transcription (Table 2.2) (NEB LUNA Reverse Transcription Kit), following the manufacturer's protocol.

Total RNA was extracted using a Monarch (New England Biolabs) RNA miniprep kit, and concentrations and purity were quantified using a Nanodrop spectrophotometer. A total of 250 ng of RNA was used for reverse transcription (NEB LUNA Reverse Transcription Kit), following the manufacturer's protocol. To perform the qPCR, LUNA SYBR Green master mix (NEB) was used. Each reaction contained the following: 0.5 µM of both forward and reverse primers (Table 2.3), 2 µL of DNF template (appropriately diluted), 2x 10 µL of qPCR master mix and the remaining volume was made up of nuclease-free ddH_2O.

The next stage is thermal cycling. A real-time qPCR was performed using stranded thermal cycling conditions consisting of denaturation at 94-98°C, annealing at 50-65°C, and extension at 72°C. Denaturation separated double-stranded DNA, and annealing then allowed primers to bind to complementary target sequences (Table 2.3). This accurate binding of primers is what initiates the DNA synthesis and ensures amplification occurs in the correct region. Extension is where the temperature increases (72°C), and primer binds to the Taq polymerase enzyme, synthesising new DNA. DNA replication occurred at this stage as new double-stranded DNA is

generated. Generally, all the above steps are repeated approximately 25 to 30 times. The longer the run time, the greater the amplified DNA.

To perform the qPCR, LUNA SYBR Green master mix (NEB) was used, and each reaction contained the following: 0.5 µM of forward and reverse primers (Table 2.3 & 2.4), 2 µL of cDNA, 5 µL of 2x qPCR master mix and the remaining volume was made up of nuclease-free ddH_2O. qPCR was performed using a Roche LightCycler following the manufacturer's instructions (Table 2.5).

Thermal cycling conditions used for quantitative polymerase chain reaction (qPCR). The initial step was denaturation, followed by 45 cycles of amplification comprising denaturation and annealing/extension.

Table 2.2: Reverse Transcription Conditions

CYCLE STEP	TEMPERATURE	TIME
PRIMER ANNEALING	25°C	2 minutes
CDNA SYNTHESIS	**55°C**	**10 minutes**
HEAT INACTIVATION	95°C	1 minute

Table 2.3: Complementary Primer sequences used for qPCR

	Primer (5'-3')	
	Forward	**Reverse**
L19	GCAGCCGGCGCAAA	GCGGAAGGGTACAGCCAAT
KLK2	CCTCACGTTCTGGCATCACTT	CGGCCAGGTGAGTTCCAA
NDRG1	GCAGCACACACTTCACAAAGC	CCAGGCACCCGTTTGAAC

Table 2.4: Annealing positions within target genes

Gene	CDS Region Amplified (bp)	Approx. Amplicon Size (bp)
L19	240-316	77
KLK2	828-895	68
NDRG1	1497-1562	66

Table 2.5 – Reaction conditions for qPCR

STEP	TEMPERATURE	TIME	CYCLES
INITIAL DENATURATION	95 °C	1 minute	1
AMPLIFICATION			45
DENATURATION	95 °C	15 seconds	
ANNEALING/EXTENSION/READ	60 °C*	30 seconds	
MELT CURVE ANALYSIS	Instrument Default	Instrument Default	1

2.6 Mutagenesis (DNA)Sequencing

Site-directed mutagenesis was performed using an Agilent QuickChange II kit, following the manufacturer's protocol. Primer sequences were designed using the Agilent Primer Design Tool: forward 5'-ttccagcggttagaatggcgccggcc-3', reverse 5'-ggcccggcgccattctaaccgctggaa-3'. Mutagenesis products were subsequently transformed into XL1 blue *E. coli*, miniprepped and successful mutagenesis confirmed using Sanger sequencing (Eurofins).

2.7 Plasmid Maps of the TAT-GRE-E1B-LUC and TAT-STOP Constructs

The plasmid constructs used throughout this research are shown below (Figure 6). Plasmid maps of both TAT-GRE-E1B-LUC and TAT-STOP constructs were generated using SnapGene software. TAT-GRE-E1B-LUC (4863 bp) was used as the main initial androgen-responsive reporter plasmid that contains androgen response elements (AREs) upstream of the luciferase (LUC) gene to allow for measuring AR-mediated transcriptional activity.

To generate the TAT-STOP construct, it was derived from TAT-GRE-E2B-LUC through site-directed mutagenesis. This introduced a premature stop codon within the luciferase (LUC) sequence while maintaining all other remaining regulatory sequences and plasmid formation. These constructs were next introduced into the reporter assays to investigate the effect of the inserted stop codon on the overall reporter output and AR signalling.

(a) (b)

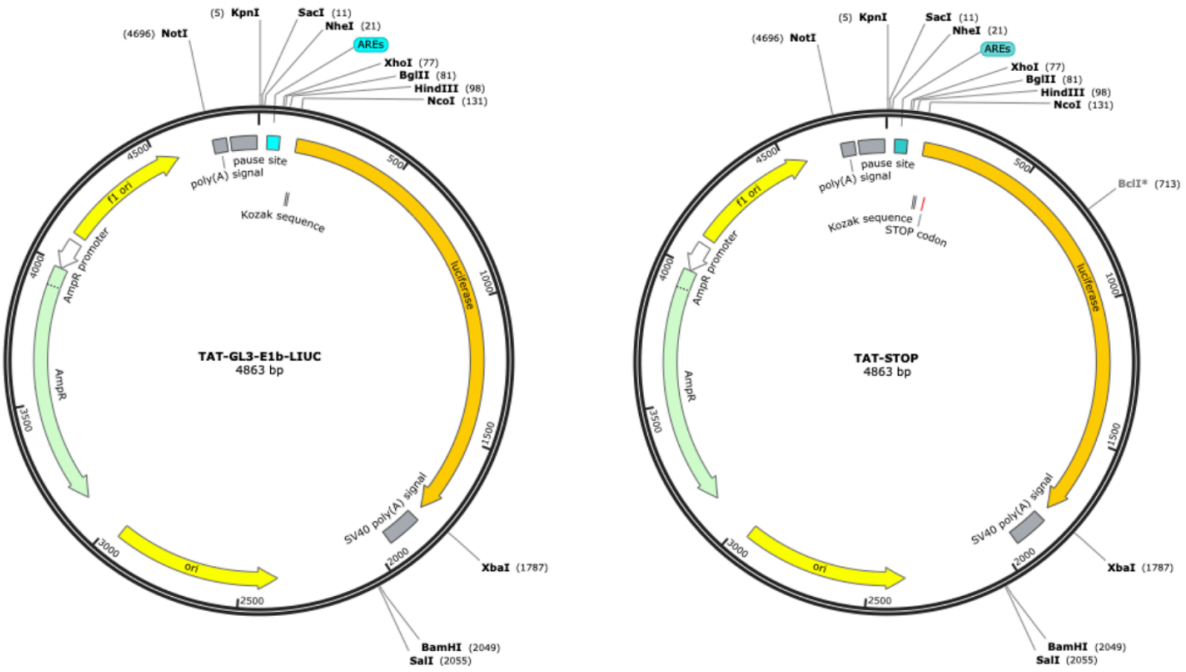

Figure 6: TAT-GRE-E1B-LUC and TAT-STOP construct plasmid maps

Illustrating TAT-GRE-E1B-LUC and TAT-ATOP plasmid maps. (a) TAT-GRE-E1B-LUC reporter plasmid containing androgen response elements (AREs) positioned before the luciferase (LUC) gene to enable AR transcriptional activity. (b) TAT-STOP construct containing an inserted stop codon sequence designed to interfere with reporter activity. Both plasmid maps have a total of 4863 bp and contain regulatory regions and the restriction enzyme sites.

2.8 DNA Nanoflowers Production

DNAzyme nanoflowers were synthesised using rolling circle amplification (RCA). The hybridisation reaction mixture was prepared by combining the primer (Table 2.7) and oligonucleotides in the reaction buffer at a final concentration of 1.2 µM and 0.6 µM, respectively. The mixture was heated to 95°C for 5 minutes and then cooled gradually to RT over 3 hrs. T4 DNA ligase (Thermo Fisher) was subsequently added, and the reaction was incubated at RT for a further 4 hrs.

The RCA reaction was set up by combining the hybridisation mix DNA with Phi29 DNA polymerase, dNTPs (2 mM final concentration), BSA, and the reaction buffer, along with the FITC-labelled dUNTPs to allow for fluorescent labelling. Amplification was performed at 30°C for 2, 4, 8, or 16 hours.

Following amplification, the samples were centrifuged at 5000 × g at 4°C for 30 minutes. The resulting pellets were washed twice with distilled water (ddH_2O) and resuspended. 1 µl of each sample was placed onto a microscope slide and visualised using an EVOS-FL fluorescence microscope.

Table 2.6 Complementary sequences used for DNAzyme nanoflower (DNF) synthesis (5'-3').

DNF Primer (+)	5'-CAC AAC CAC CAC CAC CCC ACC ACC AC-3'
DNF Primer (-)	5'- GTG GTG GTG GGG TGG TGG TG-3'
Direct ARE DNF	5'- /5Phos/ CAC AAC CAC CAC CAC CAA GGT TCT TGG AGT ACT AAG GT CTT GGA GTA CTA AGG TTC TTG GAG TAC GGT TCT TGG AGT ACT CCA CCA CCA C -3'
Palindromic AR DNF	5'- /5Phos/ CAC AAC CAC CAC CAC CAA AGA ACA TGA ACC AAA GAA CAT GAT GTA CCA AAG AAC ATG TAC CAA AGA ACA TAG TGT ACC AAC CAC CAC CAC – 3'
Aptamer	5'-CACAACCACCACCACC CCACCACCAC-3'

2.9 Transformation of Competent Cells (E.coli)

Escherichia coli XL-1 cells were transformed according to the standard protocol outlined by Promega. 50 µl of cells were thawed on ice and gently mixed with 2 µl of the mutagenesis reaction. The mixture was incubated on ice for 30 min, followed by heat shocking at 42 °C for 45 secs. The cells were then incubated on ice for a further 2 mins before the addition of 950 µl of SOC medium (table 2.1) and incubated at 37 °C for 1.5 hrs with shaking at 150 rpm. 100 µl of cell suspension was spread on an LB agar plate containing 100 μg/ml ampicillin (Table 2.1) and incubated overnight at 37 °C overnight to allow for colony growth.

Chapter 3: Results

3.1 Androgen Dose Response Curve

3.1.1 Optimisation of androgen and reporter concentrations

To identify the optimal concentration of mibolerone (synthetic non-metabolisable form of DHT) to be used for future experiments, reporter assays were performed in COS1 cells (Figure 7a). As expected, at 0 nM MIB, there was minimal AR activity, and activity increased at 10 nM MIB. There was little change in activity at the higher concentrations of mibolerone, and so, 10 nM was selected for future experiments. Western blot analysis (Figure 7b) of the AR in response to the varying mibolerone doses demonstrated that at 0 nM MIB, AR levels were low. At 10–1000 nM, MIB AR levels increased markedly.

TAT-GRE-E1B-LUC plasmid concentrations were also optimised. COS1 cells were transfected with varying concentrations of TAT-GRE-E1B-LUC reporter plasmid (0-2000 ng) and reporter assays performed (Figure 7c). As expected, following MIB treatment, increasing concentrations of TAT-GRE-E1B-LUC resulted in increasing reporter activity, with the highest luciferase signal observed at 2000ng of plasmid. This likely reflects increased reporter availability rather than changes in intrinsic AR activity. Western blot analysis (Figure 7d) of the lysates from the reporter assays demonstrated that AR protein levels appeared to increase across conditions containing higher concentrations of reporter plasmid following androgen treatment. However, the reporter plasmid concentration is unlikely to directly influence AR expression, and the observed effect may instead reflect androgen-dependent stabilisation of AR.

AR protein levels increase as the concentration of reporter plasmid increases, and this increase was also androgen-dependent.

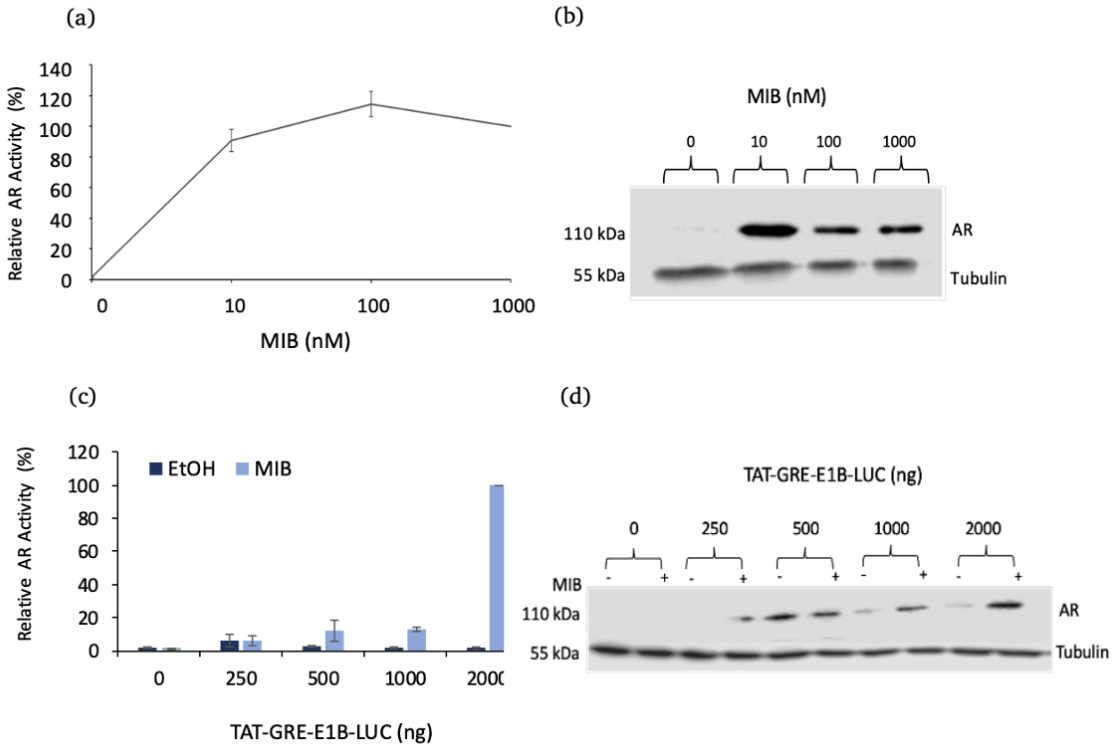

Figure 7: Optimisation of androgen and AR reporter concentrations

COS1 cells were transfected with plasmids (pSVAR/pVP16-AR), the TAT-GRE-E1B-LUC reporter plasmid, and (BOS-β-gal), as a normalisation control and treated ± 10 nM mibolerone. Graphs a and c show luciferase reporter activity normalised to β-gal is shown as mean ± SE from at least 3 independent experiments repeated in duplicate. (b and d) Representative western blots were performed and showed AR protein expression under the indicated treatment conditions.

3.2 Mutagenesis - Cloning of mutant TAT-GRE-LUC

To create a decoy binding site, mutagenesis was performed to introduce a stop codon into the TAT-GRE-E1B-LUC plasmid (termed TAT-STOP), and Sanger sequencing was performed. BLAST alignment (Figure 8a) was also performed between the mutant (Sbjct) and wild-type (Query) sequences to confirm the absence of additional mutations. BLAST verified both sequences were near identical with a single base substitution (highlighted in red) towards the 3' prime end of the sequence. The premature stop codon was inserted into the luciferase (LUC) gene at amino acid position 15. The introduced mutation generated a premature TAG stop codon, as well as verifying that no additional unwanted changes were detected, demonstrating that mutagenesis was precise and effective. The chromatogram (Figure 8b) highlights the wild-type (top) and stop codon mutant (bottom) DNA sequences. The mutant contains a successfully inserted TAG stop codon at the desired region, confirming successful site-directed mutagenesis.

The stop codon was introduced to prevent the reporter plasmid from producing a functional output while maintaining the androgen receptor binding site. This allowed the plasmid construct to act as a competitive decoy rather than producing downstream luciferase activity.

(a)

Sequence used to obtain the mutagenesis

Sequence ID: Query_965235 **Length:** 399 **Number of Matches:** 1

Range 1: 43 to 343 Graphics ▼ Next Match ▲ Previous Match

Score	Expect	Identities	Gaps	Strand
551 bits(298)	6e-161	300/301(99%)	0/301(0%)	Plus/Minus

```
Query  1    TTTCACTGCATACGACGATTCTGTGATTTGTATTCAGCCCATATCGTTTCATAGCTTCTG  60
            ||||||||||||||||||||||||||||||||||||||||||||||||||||||||||||
Sbjct  343  TTTCACTGCATACGACGATTCTGTGATTTGTATTCAGCCCATATCGTTTCATAGCTTCTG  284

Query  61   CCAACCGAACGGACATTTCGAAGTACTCAGCGTAAGTGATGTCCACCTCGATATGTGCAT  120
            ||||||||||||||||||||||||||||||||||||||||||||||||||||||||||||
Sbjct  283  CCAACCGAACGGACATTTCGAAGTACTCAGCGTAAGTGATGTCCACCTCGATATGTGCAT  224

Query  121  CTGTAAAAGCAATTGTTCCAGGAACCAGGGCGTATCTCTTCATAGCCTTATGCAGTTGCT  180
            ||||||||||||||||||||||||||||||||||||||||||||||||||||||||||||
Sbjct  223  CTGTAAAAGCAATTGTTCCAGGAACCAGGGCGTATCTCTTCATAGCCTTATGCAGTTGCT  164

Query  181  CTCCAGCGGTTCCATCTTCCAGCGGTTAGAATGGCGCCGGGCCTTTCTTTATGTTTTTGG  240
            ||||||||||||||||||||||||||||||||||||||||||||||||||||||||||||
Sbjct  163  CTCCAGCGGTTCCATCTTCCAGCGGATAGAATGGCGCCGGGCCTTTCTTTATGTTTTTGG  104

Query  241  CGTCTTCCATGGTGGCTTTACCAACAGTACCGGAATGCCAAGCTTACTTAGATCGCAGAT  300
            ||||||||||||||||||||||||||||||||||||||||||||||||||||||||||||
Sbjct  103  CGTCTTCCATGGTGGCTTTACCAACAGTACCGGAATGCCAAGCTTACTTAGATCGCAGAT  44

Query  301  C  301
            |
Sbjct  43   C  43
```

KEY: Query = wild-type sequence, Sbjct = STOP sequence

(b)

Wild-type (TAT-GRE-E1B-LUC)

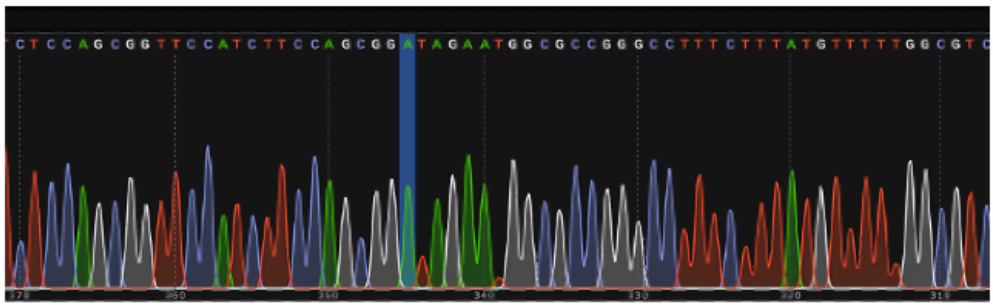

Mutant (Stop Codon/TAT-STOP)

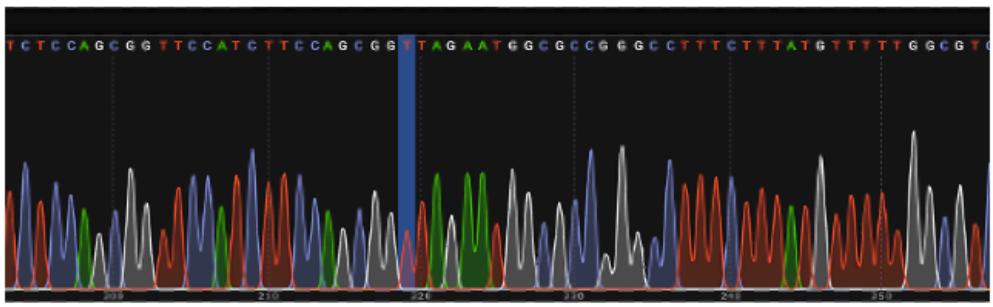

Figure 8: Confirmation of specific site-directed mutagenesis sequence for Stop Codon insertion.

a) BLAST alignment of the Query (wild type) and the Sbjct (mutated stop codon) sequences. b) Displays successful mutagenesis of a premature stop codon. The wild-type DNA sequence (top) and the mutated DNA sequence (bottom) are displayed, with the mutation site clearly visible.

3.3 Confirmation of Stop Codon Activity

Luciferase reporter assays were conducted to quantify AR activity in response to increasing concentrations of mibolerone (MIB) using wild-type TAT-GRE-E1B-LUC and mutant TAT-STOP reporter plasmids. In the wild-type construct (Figure 9a), AR activity was increased in response to 0.1 nM MIB, and increasing concentrations had little impact on this activity. Western blot analysis (Figure 9b) confirmed AR expression across all MIB concentrations.

In contrast, TAT-STOP showed no detectable luciferase activity across all MIB concentrations (Figure 9c), which is consistent with successful disruption of reporter expression and function following stop codon insertion rather than loss of androgen receptor function. Western blotting (Figure 9d) confirmed AR protein presence at ~110 kDa, validating successful transfection despite the lack of reporter output.

A schematic comparison of both constructs is shown in Figure 9e. The wild-type TAT-GRE-E1B-LUC reporter plasmid contains functional ARE elements and a luciferase

gene, allowing for quantification of AR activity via luciferase signal. Whereas the mutant TAT-STOP reporter plasmid construct contains the same regulatory functional elements as TAT-GRE-E1B-LUC but includes a premature stop codon within the luciferase coding sequence, thereby eliminating reporter activity irrespective of AR binding.

Together, these results confirm that the TAT-STOP construct successfully interfered and prevented functional luciferase activity while maintaining the modified construct for further investigation for its potential use as a competitive AR decoy.

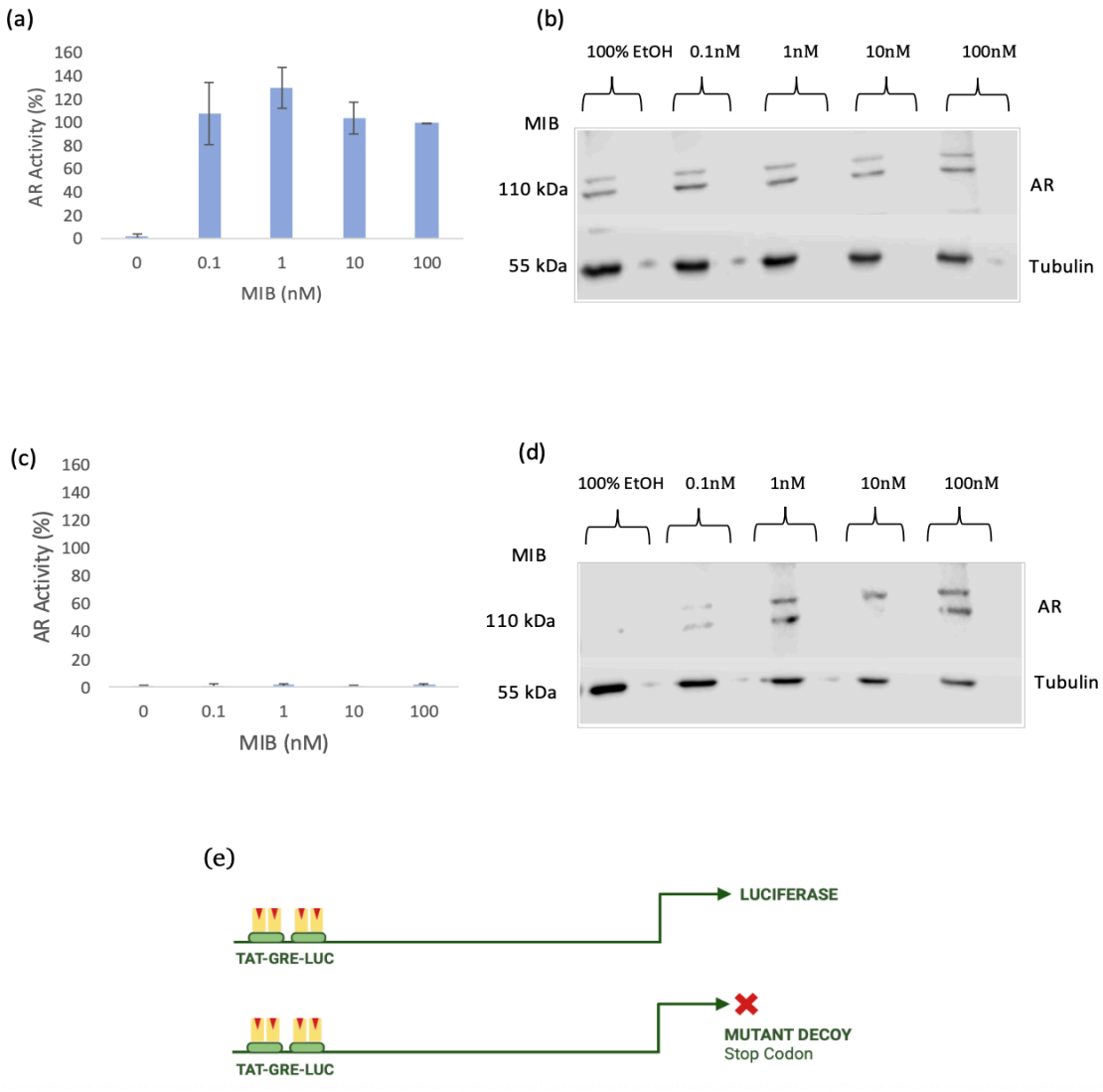

Figure 9: Confirmation that the introduction of the stop codon blocks luciferase activity.

COS1 cells were transfected with pSVAR and with either wild-type TAT-GRE-E1B-LUC reporter construct, or the mutant TAT-STOP construct and treated with increasing MIB concentrations (0,0.1,1,10 and 100 nM). (a) Luciferase reporter activity of the wild-type TAT-GRE-E1B-LUC construct was normalised to β-gal and expressed relative to the response observed at 100nM MIB (100% activity). (c) Luciferase reporter activity of the TAT-STOP construct was normalised to β-gal and expressed relative to the response at 100nM MIB. An average of at least 3 independent experiments repeated in duplicate. Mean ± SE (b and d) Western blots were performed to visualise AR levels in response to the different treatments.

3.4 Inhibition of the androgen receptor with decoy site

To determine whether the introduction of a premature stop codon within the luciferase (LUC) sequence altered the reporter output while maintaining AR protein detection luciferase reporter assays and western blot analysis were performed following both MIB and EtOH treatment.

Figures 10a and 10c compare the reporter output in the presence and absence of the TAT-STOP construct at concentrations of 250ng and 500ng. Samples without the stop codon showed reporter activity at approximately ~100%, whereas samples with the TAT-STOP plasmid were shown to have a reduced reporter output (~80% at 250 ng and ~70% at 500 ng). The introduction of the stop codon into the luciferase (LUC) plasmid rather than the androgen receptor sequence; these results are interpreted as

altered reporter function rather than direct inhibition of androgen receptor transcriptional activity.

Western blot analysis of both conditions, TAT-STOP (with stop codon) and TAT-GRE-E1B-LUC (without stop codon), was performed to assess whether differences in reporter output were complemented by changes in androgen receptor detected (figures 10b and 10d). AR protein was detected and measured at ~110 kDa, and tubulin at ~55 kDa across conditions. Although a minor variation in AR band intensity was observed. There was no clear reduction in AR protein levels identified following the introduction of TAT-STOP. These results suggest that the observed changes in the reporter output were not driven by altered AR protein levels.

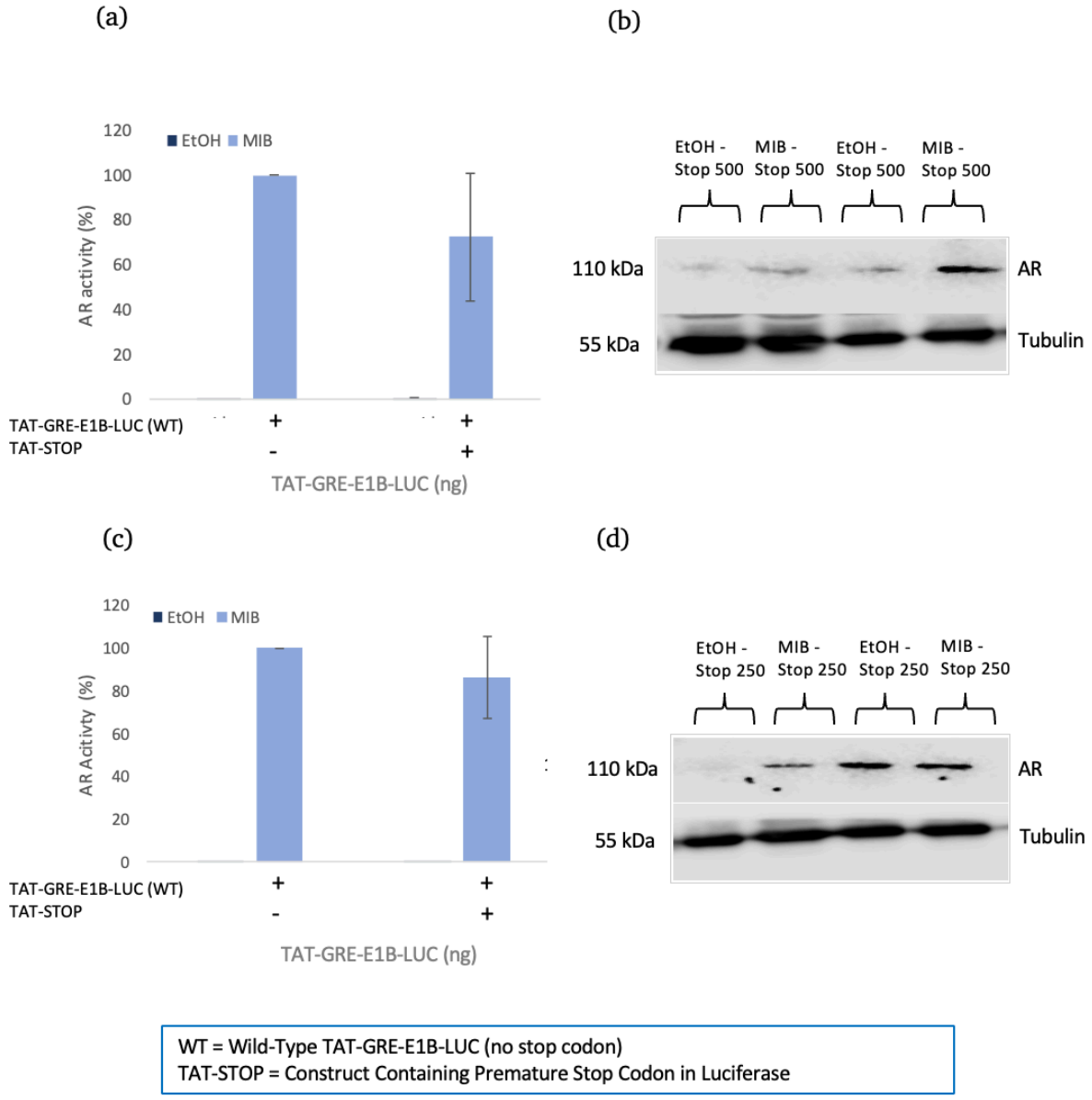

Figure 10: Graphs showing the results of inserting a stop codon.

The premature stop codon (TAT-STOP) in the TAT-GRE-E1B-LUC wild type reporter plasmid on androgen receptor protein expression, together with the presence or absence of mibolerone (MIB). The comparison of both constructs "with stop (+)" and "without stop (-)" can be visualised across two different experimental conditions. (a and c) Reporter assays were performed, and luciferase data were normalised to β-gal. Average of at least 3 independent experiments repeated in duplicate. Mean ± SE (b

and d) Western blots were performed to visualise AR levels in response to the different treatments

3.5 Effect of TAT-STOP Co-transfection on TAT-GRE-E1B-LUC reporter output

The previous experiments were performed to see if the TAT-STOP plasmid could be successfully used as a decoy but failed to show any inhibitory effect. It was hypothesised that this could be a result of too much TAT-GRE-E1B-LUC reporter plasmid being used in those experiments. To minimise this, I decided to use pVP16-AR (AR tagged with the potent VP16 transactivation domain) to assist boost androgen signalling in the presence of reduced amounts of TAT-GRE-E1B-LUC.

To investigate the influence of stop codon (TAT-STOP) on androgen receptor activity, reporter assays were performed. COS1 cells were transfected with plasmids pVP16-AR (50ng), together with TAT-GRE-E1B-LUC reporter and increasing concentrations of TAT-STOP (0-1000ng). In the absence of TAT-STOP, MIB stimulated maximum AR activity. Progressive addition of TAT-STOP (250-1000ng) was associated with a steady decline in luciferase output, with activity reduced to ~20% at 1000 ng. This reduction reflects loss of function reporter expression following stop codon insertion rather than direct suppression of AR transcriptional activity (Vanaja et al., 2002).

Western blot analysis was performed to determine whether the reduced reporter activity reflected altered AR protein expression (Figure 11b). AR was detected in the presence and absence of androgen (EtOH and MIB). AR expression was consistently detected across all plasmid concentrations and remained relatively consistent across

all conditions, although minor variation in AR was observed following MIB treatment. As the transfected AR plasmid was not directly androgen responsive, these differences were not considered to reflect the changes in AR expression and may instead be due to the transfected AR plasmid not being directly androgen responsive. These differences were not considered to reflect changes in androgen expression and may instead be explained by experimental variability and differences in transfection efficiency. This may reflect some ligand-induced stabilisation of the AR, whereby androgen binding reduces receptor turnover and degradation, leading to increased accumulation of detectable AR protein. Despite the distinct decline in luciferase activity observed in Figure 11a, tubulin expression remained uniform, confirming equal loading. Although AR protein levels showed some variation across treatment conditions and appeared to stabilise in response to MIB, these changes did not reflect the marked reduction in reporter output. This suggests that the reduced luciferase signal cannot be explained solely by changes in AR protein abundance and is consistent with altered reporter function following introduction of the TAT-STOP construct containing a premature stop codon within the luciferase (LUC) gene.

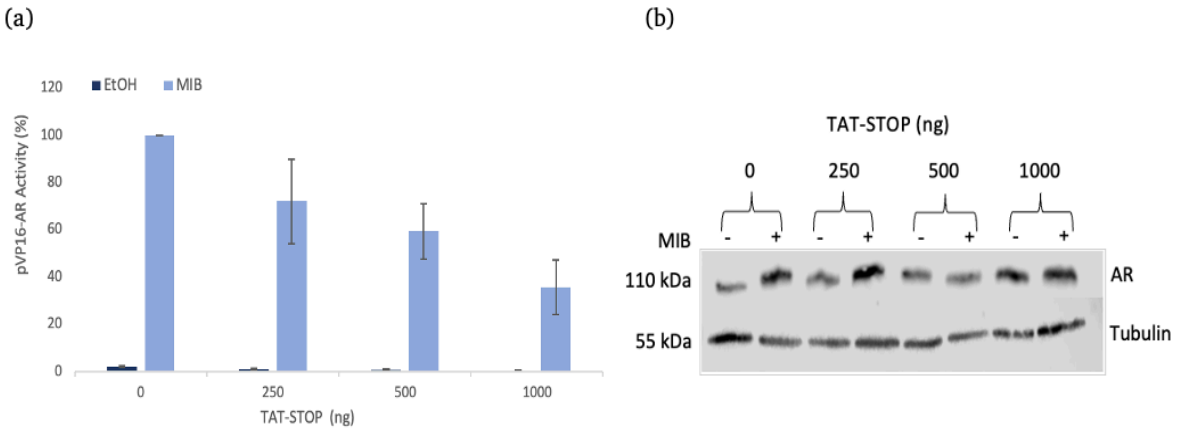

Figure 11: TAT-STOP successfully inhibits AR activity

COS1 cells were transfected with a constant concentration of TAT-GRE-E1B-LUC and pVP16-AR (50ng) and increasing concentrations of TAT-STOP (0-1000ng). Cells were treated with EtOH (vehicle control) or MIB (10 nM). (a) Reporter assays were performed, and luciferase data were normalised to β-gal. Average of at least 3 independent experiments repeated in duplicate. Mean ± SE (b) Western blots were performed to visualise AR levels in response to the different treatments.

3.6 TAT-STOP inhibits AR activity in, and the proliferation of, 22RV1 cells

3.6.1 TAT-STOP inhibits 22RV1 proliferation

To see if TAT-STOP could inhibit endogenous AR, experiments were performed in the AR-positive 22RV1 cell line. Initially, fluorescence microscopy was performed to assess transfection efficiency in 22RV1 cells (Figure 12a). GFP fluorescence indicated sufficient and high levels of transfection efficiency. The efficiency was considered to

be sufficient for the following experiments investigating the effect of the TAT-STOP construct upon AR activity and cell proliferation.

To assess the impact of TAT-STOP upon 22RV1 proliferation, cells were transfected with TAT-STOP or an empty plasmid, and to minimise background androgen signalling, all proliferation experiments were performed in stripped media before EtOH or MIB treatment. Cells were co-transfected with pEGFP-C1 so that the proliferation of transfected cells could be monitored. Fluorescence microscopy confirmed successful transfection across both treatment groups through GFP-positive cell detection (Figure 12b). Comparable GFP signal was observed across conditions, indicating that transfection efficiency was sufficient for analysis of cell proliferation. However, GFP expression was not used as a measure of androgen activity or cell growth. Importantly, the number of GFP-positive cells also remained low in TAT-STOP plasmid–transfected cells following MIB treatment, indicating that the TAT-STOP construct effectively inhibits AR-mediated proliferation despite AR stimulation.

Live-cell proliferation analysis supported these microscopy findings and was used to assess the effect of TAT-STOP on 22RV1 cell growth (Figure 12c). MIB treatment promoted proliferation in cells transfected with the empty plasmid, with increased confluency observed between 24 and 96 hours. In contrast, cells transfected with TAT-STOP showed significantly reduced proliferation following MIB treatment. EtOH-treated cells showed minimal proliferation regardless of the plasmid transfected. Collectively, these results suggest that TAT-STOP disrupts AR signalling, resulting in reduced AR-dependent transcription and cell proliferation in 22RV1 cells.

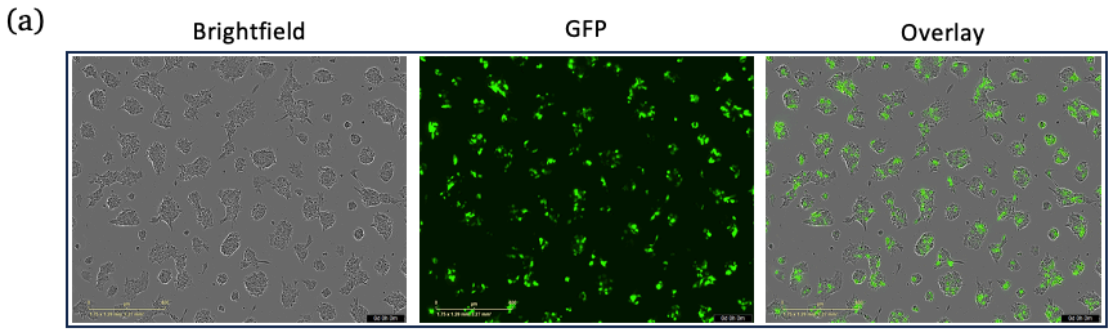
(a)
Brightfield
GFP
Overlay

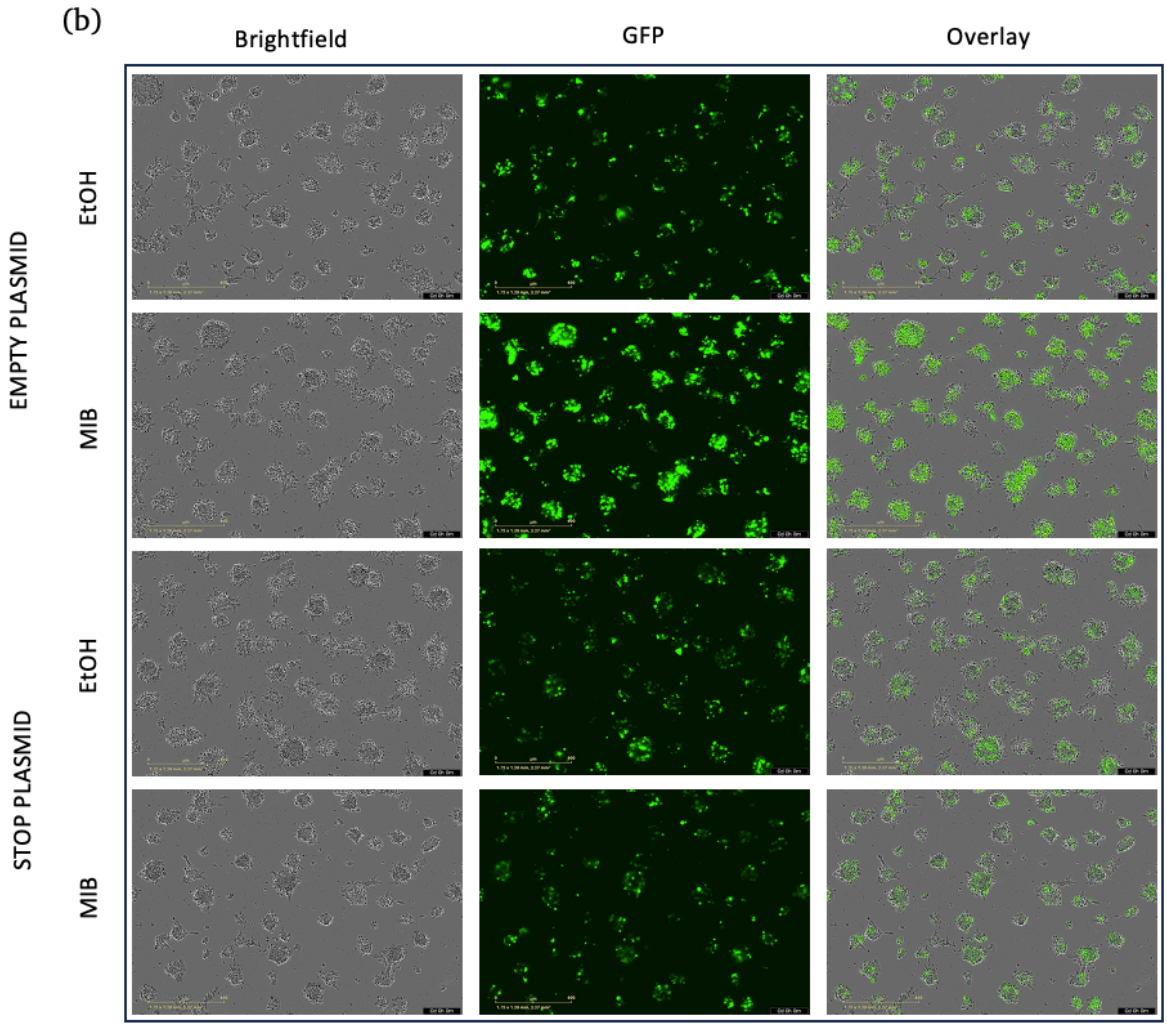
(b)
Brightfield
GFP
Overlay
EMPTY PLASMID
STOP PLASMID
EtOH
MIB
EtOH
MIB

(c)

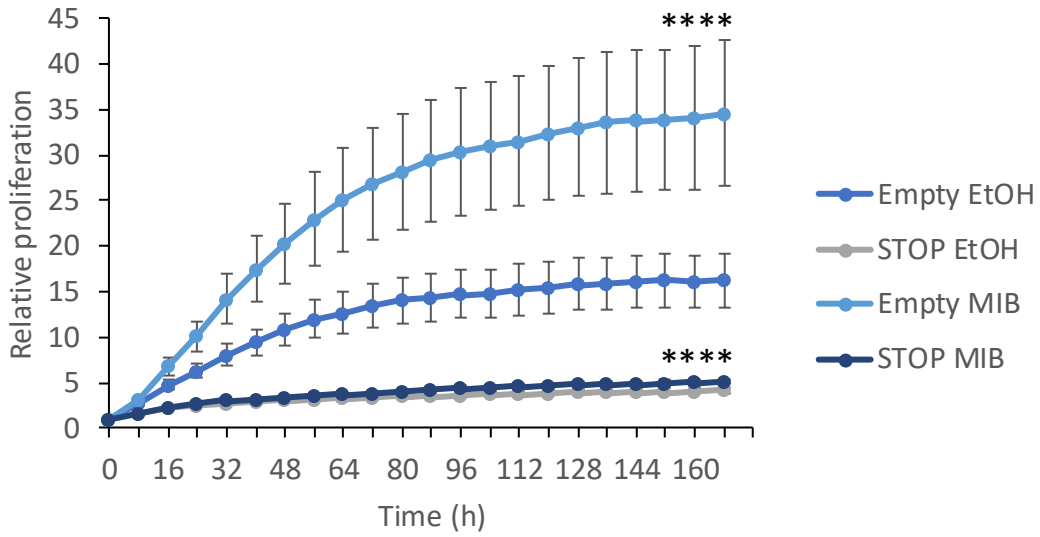

Figure 12: TAT-STOP inhibits the proliferation of 22RV1 cells.

(a) 22RV1 cells were transfected with pEGFP-C1-Empty and imaged using an IncuCyte Cell Imaging system to quantify transfection efficiency. 22RV1 cells were seeded in hormone-depleted media and transfected with pEGFP-C1 Empty ± pSG5-Empty/TAT-STOP and treated with ethanol (EtOH) or mibolerone (MIB). IncuCyte imaging was performed to (b) visualise the cells at 168 hours and (c) quantify the changes in proliferation. Mean ± SE. ANOVA **** $p<0.0001$.

3.6.2 TAT-STOP inhibits AR activity in 22RV1 cells

I have demonstrated that the TAT-STOP construct inhibits the proliferation of 22RV1 cells. To determine whether this growth inhibition is associated with reduced AR activity, qPCR analysis was performed to assess the expression of AR target genes (*KLK2* and *NDRG1*). In this analysis, L19 was used as a reference gene to normalise target gene expression and control for variation in RNA input and amplification efficiency (Figure 13).

Melt curve analysis was conducted to assess amplification specificity. A single, well-defined peak was observed at approximately 84 °C, indicating the generation of a specific PCR product with no evidence of non-specific amplification or primer-dimer formation.

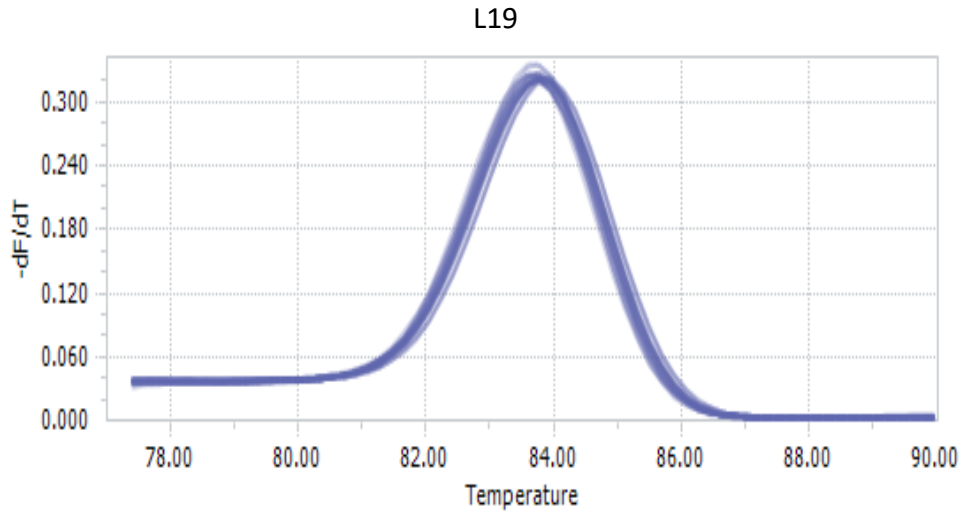

Figure 13: Melt curve analysis for housekeeping gene L19.

22RV1 were transfected with TAT-STOP or an empty plasmid control, and RNA was extracted. Reverse transcription was performed, followed by qPCR. A melt curve was performed to confirm L19 primer specificity, to be used as a normalisation control.

Melt curve analysis also confirmed amplification specificity for both AR target genes (Figure 14 a and c), with a single distinct peak observed for each reaction, indicating generation of a single specific amplicon and absence of non-specific amplification. Expression analysis showed that MIB treatment increased *KLK2* expression in cells transfected with the pSG5-EMPTY plasmid compared with EtOH controls (Figure 14b), consistent with androgen-induced AR activation, although this did not reach significance. In contrast, cells transfected with the TAT-STOP plasmid exhibited only a modest increase in KLK2 expression following MIB treatment, indicating impaired AR-dependent transcription in the presence of the decoy construct.

Similarly, in pSG5-EMPTY–transfected cells, MIB treatment resulted in a marked increase in *NDRG1* expression (Figure 14d), again consistent with AR activation. However, MIB had little to no effect on NDRG1 expression in cells transfected with the mutant TAT-STOP plasmid, suggesting effective inhibition of AR-mediated transcription. Collectively, these data suggest that the mutant TAT-STOP construct acts as a competitive decoy for AR binding, resulting in reduced AR- mediated target gene expression.

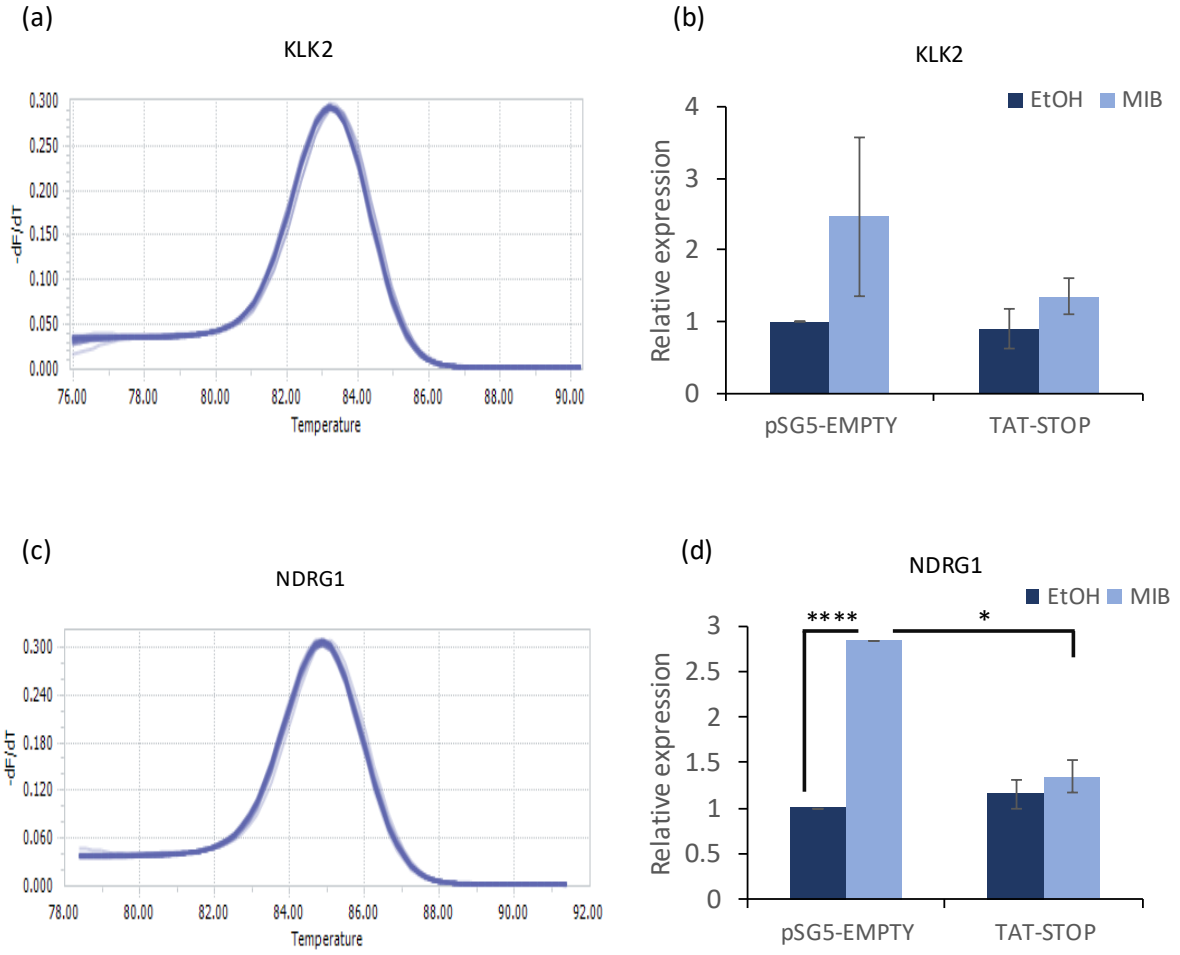

Figure 14: The TAT-STOP decoy inhibits AR activity in 22RV1 cells.

22RV1 cells were seeded in hormone-depleted (stripped) media, transfected with TAT-STOP or an empty plasmid control, and treated with EtOH or MIB. RNA was extracted, and reverse transcription was performed, followed by qPCR. Melt curves were performed for (a) *KLK2* and (b) *NDRG1*. The delta Ct method (normalised to L19 and made relative to EtOH) was used to calculate the change in (c) *KLK2* and (d) *NDRG1* expression in response to the different constructs and ethanol (EtOH) or mibolerone (MIB). Mean ± SE from an average of at least 3 independent experiments, with each treatment condition transfected across 4 wells (N=4 per condition). Statistical significance was determined using ANOVA * $p<0.05$,

****$p<0.0001$. ANOVA was used because comparing 4 different treatment conditions across multiple times. This allowed for a multiple comparison test.

3.6.3 Nanoflower Construction and EVOS Imaging

I have successfully demonstrated that decoy binding sites can inhibit AR activity in 22RV1 cells. To investigate this approach into a potential delivery platform, the AREs decoy sequences derived from the TAT-GRE-E1B-LUC and TAT/STOP constructs were incorporated into the circular templates for the DNA nanoflower synthesis. This allowed for repeated appearance of AR-binding motifs following the rolling chain amplification (RCA). However, to translate this strategy towards a therapeutic that can be used clinically, an effective method for *in vivo* delivery is required. To address this, I investigated the potential of DNA nanoflowers (DNFs) as a delivery system for AR decoy binding sites.

Fluorescence microscopy using EVOS imaging was employed to assess the generation of fluorescently labelled DNFs at multiple time points of rolling circle amplification (2, 4, 8, and 16 hours) (Figure 15a). Green fluorescence indicates the presence of DNFs. Across experimental conditions, an increase in fluorescence intensity was observed from earlier to later time points, suggesting time-dependent generation of the DNFs. As part of the DNF optimization, two circular template designs containing either a direct or palindromic AREs were investigated to assess whether repeat alignment influenced DNF synthesis and formation efficiency (Table 2.6). The top row of images represents DNFs containing direct androgen response elements (AREs), while the bottom row represents palindromic ARE DNFs. Optimal rolling circle

amplification appeared to be 8 hours, and hence this was selected for future experiments. However, despite this initial success, future experiments that aimed to generate DNFs failed. Several optimisations (Table 2.7) were made, but none of these changes led to the successful generation of DNFs containing decoy binding sites. I was therefore unable to test the efficacy of this delivery method in cells.

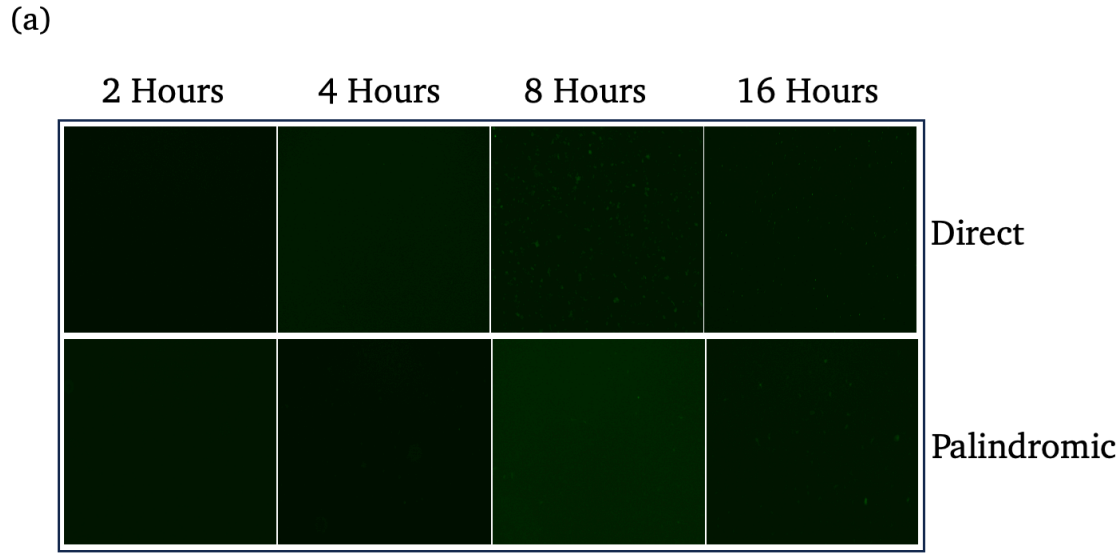

Figure 15: DNAzyme nanoflower (DNFs) synthesis at varying rolling circle amplification (RCA) times using f-12-dUTPs.

Fluorescein- labelled dUTPs (f-12-dUTPs) were incorporated during RCA to allow fluorescent detection of DNF synthesis.

DNF constructs were designed containing either direct or palindromic AREs. The oligos were initially annealed, and then rolling circle PCR was performed at different timepoints. Successful DNF production was assessed using EVOS FL imaging.

Table 2.7. Optimisation attempted for DNF production.

Several optimisations (different reagents) were attempted to resolve the issues with the DNF production. The changes made are summarised in the table.

Attempted	Outcome	Changed	Outcome
T4 DNA Ligase (New England Biolab)	Unsuccessful	T4 DNA Ligase (Thermo Fisher Scientific)	Unsuccessful Changed back to biolabs
dNTPs (Thermo Fisher Scientifuc)	Unsuccessful	dNTPs (Applied Biosystems)	Unsuccessful
Phi29 DNA Polymerase (10U/μl) - (New England Biolab) Old Sample	Unsuccessful	Phi29 DNA Polymerase (10U/μl) - (New England Biolab) New Sample	Unsuccessful

Chapter 4: Discussion

The main aim of this project was to assess and test whether exogenous AREs could be used as a decoy to disrupt and block AR activity. The ARE sequences used in these experiments mimic the natural DNA regions that AR generally and naturally binds to. This ARE based decoy strategy involves using DNA sequences comprising of both direct and palindromic repeat AREs as decoys. The hypothesis was that the AR would bind to the decoy AREs, preventing it from binding to its original intended target gene. The structural organisation of the direct repeat and palindromic repeat androgen response element (ARE) decoy design used in this study is shown in (Figure 15. This strategy is also hypothesised to be able to inhibit AR activity regardless of any mechanisms of resistance, for example, AR mutations and variants will be inhibited by the decoy. This approach works by interfering with its (the ARs) ability to bind DNA, making it a useful approach for cancers that have become resistant to novel mainstream treatments. Irrespective of AR mutations, DNA binding still occurs to activate genes, which is where the AREs decoys step in to block this process from happening.

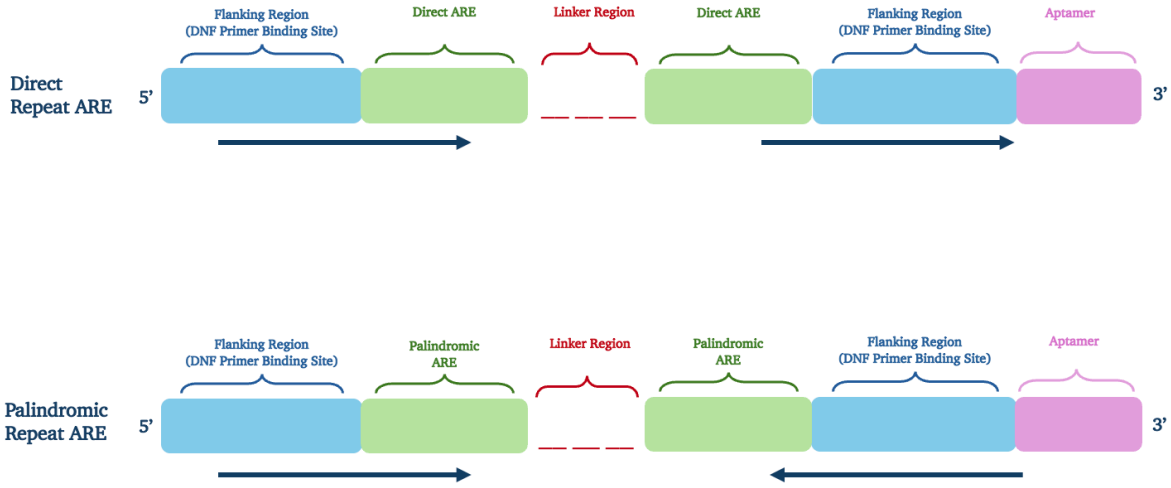

Figure 16: Schematic of direct and palindromic androgen response element (ARE) decoy design and structure.

Direct repeat AREs are arranged in the same orientation. whereas palindromic repeat AREs are arranged in opposing orientation. The blue region represents flanking regions; the green regions represent the ARE decoy site; the red regions represent linker sequences; and the pink region represents the aptamer sequence. The arrows indicate the sequence orientation across each repeat construct.

The experimental results support this theory, as demonstrated by both AR protein expression analysis and in luciferase reporter assays. The introduction of the ARE based decoys significantly inhibited AR activity. These findings indicate that ARE based decoy effectively interfere with the androgen receptors and reduce transcriptional activity, as shown in the luciferase (LUC) assays.

The reduction in reporter output with TAT-STOP reflects the expected results of an inserted stop codon, and overall luciferase activity was noticeably reduced due to luciferase translation.

Western blot analysis further confirmed that following co-transfection with the decoy constructs, AR protein levels remained mainly unchanged despite reduced reporter output. This supports the conclusion that ARE decoys can successfully inhibit AR signalling through competition for DNA binding rather than changes in AR protein levels.

It is known that AR can be mutated or truncated into different variants, for example, AR-V7 (Haile and Sadar, 2011); a shortened version of AR which remains transcriptionally active but does not require androgen to be active. Importantly, even these resistant AR versions still require DNA binding to occur for target gene regulation. The ARE decoys work by competing with the androgen response elements for AR binding. Diverting the AR away from its standard target sequences and reducing activation of target genes. This approach still targets the DNA-binding that is shared by the mutant AR forms. ARE decoys may act as a potential therapeutic strategy, which could therefore be useful in treating a range of mechanisms that promote therapy-resistant disease.

These results are consistent with previous work demonstrating that synthetic DNA constructs mimicking AREs can act as competitive inhibitors of transcription factors. Studies such as (Dehm and Tindall, 2011) (S.N. Quayle N.R. Mawji, 2007)have

identified that decoy oligonucleotides containing AREs can inhibit AR transcriptional activity in prostate cancer.

Transfection of the TAT-STOP construct into 22RV1 cells, which expresses both full-length and variant AR, provided evidence that this approach is functionally effective in inhibiting variant and full-length AR activity and prostate cancer growth. Further experiments were conducted to gain a broader understanding of the impact of the decoy constructs on AR transcriptional function. For further experimental trials, a wider range of AR target genes could be analysed/RNA sequencing (RNA-seq) could be performed to capture the overall AR inhibition. Additionally, chromatin immunoprecipitation (ChIP) assays can be performed to confirm loss of AR binding to AR target genes.

The TAT-STOP construct was assessed in the 22RV1 cell proliferation experiments. Therefore, it was not possible to determine of TAT-GRE-E1B-LUC would produce similar results on the cell growth or if the reporter output corresponds directly with reduced proliferation. Further experiments would need to be performed to investigate this relationship.

DNA nanoflowers (DNFs) were investigated as a potential delivery method for the decoys and initially showed promising formation. However, further synthesis attempts produced inconsistent results despite multiple optimisation steps and repeats. As a result, it was evident that the production of DNFs was not viable or consistent, preventing further functional experiments to assess delivery efficacy.

Future work should focus on optimising the DNFs, or alternative strategies should be investigated (Yi Jin, 2017, Henriquez et al., 2021).

An alternative to DNFs could be to use a more conventional nanoparticle-based delivery method. Nanoparticles have many useful prospects. They help by shielding and protecting the decoy constructs from degradation (Maarifa et al., 2025). Another option could be viral delivery, which works as viruses function as carriers to deliver the decoys into cells, using the efficiency of how effectively viruses can enter the cell, releasing genetic material inside the cell (De Haan et al., 2021).

In conclusion, decoy binding sites present a good option as a promising therapeutic approach for targeting AR activity, particularly when treating resistant prostate cancer. By mimicking the AREs, these decoys can effectively inhibit AR and hinder its ability to regulate gene expression. However, the full potential of this approach comes with limitations of effective and targeted delivery. Although DNFs were explored as a potential delivery strategy for decoy constructs to be delivered into cancer cells, the continuous, inconsistent synthesis limited further functional evaluation. Further research should not only focus on optimising decoy sequences but also focus on developing strong delivery mechanisms to ensure the delivery carries through. Both components need to be in place for a successful decoy-based approach to be put into practice.

Studies have shown DNFs to be effective and successful in drug delivery. However, improvements in DNF design and structure could increase therapeutic efficacy and

DNF stability. Chemical modification, like 2'-O-methyl or phosphorothioate replacements, increases resistance degradation, thus improving stability *in vivo* (Mahboobeh Nasiri et al, 2024). Incorporating inorganic materials such as gold nanoparticles can enhance circulation time and overall function. Introducing multivalent targeting ligands on the DNFs surface can increase binding specificity and affinity towards cancer cells. (Fu and Xiang, 2020). Furthermore, adjusting the rolling circle amplification (RCA) conditions, such as reaction time, primer concentration (ng) may have a positive effect on nanoflower density, size and drug uptake capacity.

One design consideration during DNFs development was the choice of circular template sequence, including the use of both direct repeats and palindromic repeats. Choosing between which repeats would positively influence DNF synthesis and structural formation. Direct repeats are comprised of repeated linear sequences, which allow polymerase to successfully produce long single-stranded DNA without affecting the final structure. In comparison, palindromic repeat sequences form hairpins or stem-loop-like structures, which can obstruct RCA by stalling polymerase or terminating premature amplification. This hindrance can affect the uniformity of the final nanoflowers. Studies have discussed this argument of which repeats are better for DNFs. Generally, direct repeats are preferred for nanoflower synthesis, especially for the use of therapeutic applications where stability, size, and efficient drug delivery need to remain consistent.

Chapter 5: References

AULAKH, S. & MYSORE, V. 2025. Bicalutamide: A review. *J Cutan Aesthet Surg,* 18**,** 78-85.

AURILIO, G., CIMADAMORE, A., MAZZUCCHELLI, R., LOPEZ-BELTRAN, A., VERRI, E., SCARPELLI, M., MASSARI, F., CHENG, L., SANTONI, M. & MONTIRONI, R. 2020. Androgen Receptor Signaling Pathway in Prostate Cancer: From Genetics to Clinical Applications. *Cells,* 9.

BRINKMANN, A. O. 2011. Molecular mechanisms of androgen action--a historical perspective. *Methods Mol Biol,* 776**,** 3-24.

BRINKMANN, A. O., BLOK, L. J., DE RUITER, P. E., DOESBURG, P., STEKETEE, K., BERREVOETS, C. A. & TRAPMAN, J. 1999. Mechanisms of androgen receptor activation and function. *J Steroid Biochem Mol Biol,* 69**,** 307-13.

BROOKE, G. N. & BEVAN, C. L. 2009. The role of androgen receptor mutations in prostate cancer progression. *Curr Genomics,* 10**,** 18-25.

CLEUTJENS, K. B., VAN DER KORPUT, H. A., VAN EEKELEN, C. C., VAN ROOIJ, H. C., FABER, P. W. & TRAPMAN, J. 1997. An androgen response element in a far upstream enhancer region is essential for high, androgen-regulated activity of the prostate-specific antigen promoter. *Mol Endocrinol,* 11**,** 148-61.

DAHABREH, I. J., CHUNG, M., BALK, E. M., YU, W. W., MATHEW, P., LAU, J. & IP, S. 2012. Active surveillance in men with localized prostate cancer: a systematic review. *Ann Intern Med,* 156**,** 582-90.

DATTA, K., MUDERS, M., ZHANG, H. & TINDALL, D. J. 2010. Mechanism of lymph node metastasis in prostate cancer.

DAVEY, R. A. & GROSSMANN, M. 2016. Androgen Receptor Structure, Function and Biology: From Bench to Bedside. *Clin Biochem Rev,* 37**,** 3-15.

DE HAAN, P., VAN DIEMEN, F. R. & TOSCANO, M. G. 2021. Viral gene delivery vectors: the next generation medicines for immune-related diseases. *Hum Vaccin Immunother,* 17**,** 14-21.

DEHM, S. M. & TINDALL, D. J. 2011. Alternatively spliced androgen receptor variants. *Endocr Relat Cancer,* 18**,** R183-96.

FERRALDESCHI, R., WELTI, J., POWERS, M. V., YUAN, W., SMYTH, T., SEED, G., RIISNAES, R., HEDAYAT, S., WANG, H., CRESPO, M., NAVA RODRIGUES, D., FIGUEIREDO, I., MIRANDA, S., CARREIRA, S., LYONS, J. F., SHARP, S., PLYMATE, S. R., ATTARD, G., WALLIS, N., WORKMAN, P. & DE BONO, J. S. 2016. Second-Generation HSP90 Inhibitor Onalespib Blocks mRNA Splicing of Androgen Receptor Variant 7 in Prostate Cancer Cells. *Cancer Res,* 76**,** 2731-42.

FU, Z. & XIANG, J. 2020. Aptamer-Functionalized Nanoparticles in Targeted Delivery and Cancer Therapy. *Int J Mol Sci,* 21.

FUJITA, K. & NONOMURA, N. 2019. Role of Androgen Receptor in Prostate Cancer: A Review. *World J Mens Health,* 37**,** 288-295.

GALE, R. P. 2024. *Overview of Cancer* [Online]. Available: https://www.msdmanuals.com/home/cancer/overview-of-cancer/overview-of-cancer?ruleredirectid=742 [Accessed].

GANN, P. H. 2002. Risk factors for prostate cancer. *Rev Urol,* 4 Suppl 5**,** S3-s10.

HAILE, S. & SADAR, M. D. 2011. Androgen receptor and its splice variants in prostate cancer. *Cell Mol Life Sci,* 68**,** 3971-81.

HENRIQUEZ, I., SPRATT, D., GóMEZ-ITURRIAGA, A., ABUCHAIBE, O. & COUñAGO, F. 2021. Nonmetastatic castration-resistant prostate cancer: Novel agents to treat a lethal disease. *World J Clin Oncol,* 12**,** 6-12.

JIANG ZHAO, C. Z., WEIHAO WANG, CHEN LI, XUPENG MU, KEBANG HU 2022. Current progress of nanomedicine for prostate cancer diagnosis and treatment. *Biomedicine & Pharmacotherapy* Elsevier: Science direct

JIGANG LV, Y. D., PROF. ZI GU, PROF. DAYONG YANG 2020. Frontispiece: Programmable DNA Nanoflowers for Biosensing, Bioimaging, and Therapeutics. *Chemistry Europe* 26.

KARANTANOS, T., CORN, P. G. & THOMPSON, T. C. 2013. Prostate cancer progression after androgen deprivation therapy: mechanisms of castrate resistance and novel therapeutic approaches. *Oncogene,* 32**,** 5501-11.

LEE, J. J., THOMAS, I. C., NOLLEY, R., FERRARI, M., BROOKS, J. D. & LEPPERT, J. T. 2015. Biologic differences between peripheral and transition zone prostate cancer. *Prostate,* 75**,** 183-90.

MAARIFA, N. M., ISSIMAIL, F. E. M., HE, J. & MA, X. 2025. Synthesis with control of DNA nanoflowers towards biomedical applications. *Mater Today Bio,* 32**,** 101886.

MADAN, R. A. & GULLEY, J. L. 2011. Sipuleucel-T: harbinger of a new age of therapeutics for prostate cancer. *Expert Rev Vaccines,* 10**,** 141-50.

MANN, T. 1974. Secretory function of the prostate, seminal vesicle and other male accessory organs of reproduction. *J Reprod Fertil,* 37**,** 179-88.

MCEWAN, I. J. B., A .O. 2021. Androgen Physiology: Receptor and Metabolic Disorders.

MCNEAL, J. E. 1981. The zonal anatomy of the prostate. *Prostate,* 2**,** 35-49.

MURRAY, T. B. J. 2021. The Pathogenesis of Prostate Cancer.

NARAYANAN, R., MOHLER, M. L., BOHL, C. E., MILLER, D. D. & DALTON, J. T. 2008. Selective androgen receptor modulators in preclinical and clinical development. *Nucl Recept Signal,* 6**,** e010.

NIH. 2021. *What Is Cancer?* [Online]. National Cancer Institute. Available: https://www.cancer.gov/about-cancer/understanding/what-is-cancer#definition [Accessed].

PAGE, S. T., LIN, D. W., MOSTAGHEL, E. A., MARCK, B. T., WRIGHT, J. L., WU, J., AMORY, J. K., NELSON, P. S. & MATSUMOTO, A. M. 2011. Dihydrotestosterone Administration Does Not Increase Intraprostatic Androgen Concentrations or Alter Prostate Androgen Action in Healthy Men: A Randomized-Controlled Trial. *The Journal of Clinical Endocrinology & Metabolism,* 96**,** 430-437.

QUAYLE, S. N., MAWJI, N. R., WANG, J. & SADAR, M. D. 2007. Androgen receptor decoy molecules block the growth of prostate cancer. *Proc Natl Acad Sci U S A,* 104**,** 1331-6.

S.N. QUAYLE N.R. MAWJI, J. W. M. D. S. 2007. Androgen receptor decoy molecules block the growth of prostate cancer *Proc Natl Acad Sci U S A,* 104

SARANYUTANON, S., SRIVASTAVA, S. K., PAI, S., SINGH, S. & SINGH, A. P. 2019. Therapies Targeted to Androgen Receptor Signaling Axis in Prostate Cancer: Progress, Challenges, and Hope. *Cancers (Basel),* 12.

SHET, M. S., MCPHAUL, M., FISHER, C. W., STALLINGS, N. R. & ESTABROOK, R. W. 1997. Metabolism of the antiandrogenic drug (Flutamide) by human CYP1A2. *Drug Metab Dispos,* 25**,** 1298-303.

TAN, M. H. E., LI, J., XU, H. E., MELCHER, K. & YONG, E.-L. 2015. Androgen receptor: structure, role in prostate cancer and drug discovery. *Acta Pharmacologica Sinica,* 36**,** 3-23.

TOLKACH, Y., JONIAU, S. & VAN POPPEL, H. 2013. Luteinizing hormone-releasing hormone (LHRH) receptor agonists vs antagonists: a matter of the receptors? *BJU Int,* 111**,** 1021-30.

VANAJA, D. K., MITCHELL, S. H., TOFT, D. O. & YOUNG, C. Y. 2002. Effect of geldanamycin on androgen receptor function and stability. *Cell Stress Chaperones,* 7**,** 55-64.

VISAKORPI, T., HYYTINEN, E., KOIVISTO, P., TANNER, M., KEINäNEN, R., PALMBERG, C., PALOTIE, A., TAMMELA, T., ISOLA, J. & KALLIONIEMI, O. P. 1995. In vivo amplification of the androgen receptor gene and progression of human prostate cancer. *Nat Genet,* 9**,** 401-6.

WANG, T., TAGUE, N., WHELAN, S. A. & DUNLOP, M. J. 2021. Programmable gene regulation for metabolic engineering using decoy transcription factor binding sites. *Nucleic Acids Res,* 49**,** 1163-1172.

WILLIAM K. OH, M., MARK HURWITZ, MD, ANTHONY V. D'AMICO, MD, JEROME P. RICHIE, MD, AND PHILIP W. KANTOFF, MD. 2003. *Holland-Frei Cancer Medicine. 6th edition.*

YAMAOKA, M., HARA, T., HITAKA, T., KAKU, T., TAKEUCHI, T., TAKAHASHI, J., ASAHI, S., MIKI, H., TASAKA, A. & KUSAKA, M. 2012. Orteronel (TAK-700), a novel non-steroidal 17,20-lyase inhibitor: effects on steroid synthesis in human and monkey adrenal cells and serum steroid levels in cynomolgus monkeys. *J Steroid Biochem Mol Biol,* 129**,** 115-28.

YI JIN, Z. L., HUIFANG LIU, SHIZHU CHEN, FENG WANG, LING WANG, NAN LI, KUN GE, XINJIAN YANG, JINCHAO ZHANG 2017. Biodegradable, multifunctional DNAzyme nanoflowers for enhanced cancer therapy. *NPG Asia Mater* 9.

ZIRKIN, B. R. & PAPADOPOULOS, V. 2018. Leydig cells: formation, function, and regulation. *Biol Reprod,* 99**,** 101-111.

S.N. Quayle, N.R. Mawji, J. Wang, & M.D. Sadar, Androgen receptor decoy molecules block the growth of prostate cancer, Proc. Natl. Acad. Sci. U.S.A. 104 (4) 1331-1336, https://doi.org/10.1073/pnas.0606718104 (2007).